Geochemistry Geophysics Geosystems

Article

Volume 11, Number 7

10 July 2010

Q07006, doi:10.1029/2009GC003006

ISSN: 1525-2027

Published by AGU and the Geochemical Society

Rock magnetic property and paleointensity determination on historical Santorini lava flows

Simo Spassov

Department of Geophysics, Aristotle University of Thessaloniki, GR-54126 Thessaloniki, Greece

Now at Section du Magnétisme Environnemental, Centre de Physique du Globe, Institut Royal Météorologique de Belgique, 1 rue du Centre Physique, B-5670 Dourbes, Belgium (simo.spassov@oma.be)

Jean-Pierre Valet

Institut de Physique du Globe de Paris, 4 Place Jussieu, F-75252 Paris CEDEX 05, France

Despina Kondopoulou

Department of Geophysics, Aristotle University of Thessaloniki, GR-54126 Thessaloniki, Greece

Irene Zananiri

Institute of Geology and Mineral Exploration, Olympic Village, 3rd Entrance, GR-13677 Acharnae, Greece

Lluís Casas

Geomagnetism Laboratory, University of Liverpool, Oliver Lodge Building, Oxford Street, Liverpool L69 7ZE, UK

Now at Secció de Geologia, Facultat de Ciències, Universitat Autonòma de Barcelona, UAB Campus, E-08193 Bellaterra, Spain

Maxime Le Goff

Institut de Physique du Globe de Paris, 4 Place Jussieu, F-75252 Paris CEDEX 05, France

[1] Eight historical dacitic lava flows from Santorini with ages between 46 A.D. and 1950 A.D. (four of them within the past century) have been subjected to detailed rock magnetic analyses and various experiments of absolute paleointensity. Thermomagnetic measurements and acquisition of isothermal magnetization have revealed the presence of two physically distinct magnetic phases with Curie temperatures of 280°C and 500°C. In most of the samples, the second phase does not play a prominent role for the characteristic remanent magnetization, which is dominated by titanomagnetite. Magnetostatic interaction is very limited and does not considerably change upon heating. Back-field curve spectra indicate a good thermochemical stability of these dacitic lava samples, which is also supported by the absence of noticeable changes in the remanent coercive force prior heating to 450°C. Hysteresis measurements show typical pseudo-single-domain behavior without noticeable superparamagnetism. Such characteristics were favorable to conduct and to test the most widely used experimental approaches for absolute paleointensity determination. Despite a success rate of 38%, the microwave technique has provided rather scattered within-flow determinations. The results obtained from approaches involving alternating field demagnetization were biased by considerable differences between the NRM and the TRM coercive force spectra. We have also noticed that most determinations obtained by microwave heating differ from the historical field value at the site for the most recent flows. Last, techniques involving double-heating protocols were successful due to a dominant

low Curie temperature phase with a narrow grain size distribution. The results were characterized by low dispersion and were found in good agreement with the historical field.

Components: 11,900 words, 12 figures, 3 tables.

Keywords: rock magnetism; paleointensity; subaerial volcanics; Santorini; Greece.

Index Terms: 1521 Geomagnetism and Paleomagnetism: Paleointensity; 1540 Geomagnetism and Paleomagnetism: Rock and mineral magnetism; 1519 Geomagnetism and Paleomagnetism: Magnetic mineralogy and petrology.

Received 11 December 2009; **Revised** 2 April 2010; **Accepted** 18 May 2010; **Published** 10 July 2010.

Spassov, S., J.-P. Valet, D. Kondopoulou, I. Zananiri, L. Casas, and M. Le Goff (2010), Rock magnetic property and paleointensity determination on historical Santorini lava flows, *Geochem. Geophys. Geosyst.*, *11*, Q07006, doi:10.1029/2009GC003006.

1. Introduction

[2] Surprisingly, there is still limited knowledge of the geomagnetic field intensity variations that prevailed over the past centuries. Besides Bulgaria and France, Greece is the European best documented area [*De Marco et al.*, 2008], yet the period between 500 and 1100 A.D. remains poorly constrained, and the majority of results appear to be quite scattered. Burned archeological artifacts are by far the most appropriate material for studies of absolute paleointensity. A few limitations are linked to age uncertainties, particularly when the material has been dated with reference to the surrounding archeological context which may not always be exactly coeval of the last heating. Other problems are caused by restricted access to archeological objects, so that only the minimum material required for paleomagnetic analyses can be sampled. This is not always the case for volcanic historical lava flows, which frequently can be dated with reference to the nomenclature of the volcanic eruptions. However, both the temporal and the geographical distribution of data suffer from lack of site locations and from irregular and sparse volcanic activity, especially in Europe during the historical period. In contrast to archeological material, absolute paleointensities from volcanics suffer poor success rates for reasons that mostly depend on thermochemical alteration during laboratory treatment and even sometimes during cooling of the lava [*Yamamoto et al.*, 2003]. Despite this limitation [cf. *Leonhardt and Soffel*, 2002; *Valet*, 2003], the Thellier-Thellier [*Thellier and Thellier*, 1959] double heating method provides reliable field determinations, but with uncertainties that can reach up to 20% of the field value, which is not acceptable for studies exploring short time periods of rapid field changes. Many alternative techniques [*Coe*, 1967; *Shaw*, 1974; *Petrova and Bagina*, 1976; *Aitken et al.*, 1988; *Walton et al.*, 1992, 1993; *Tsunakawa et al.*, 1997; *Cottrell and Tarduno*, 2000; *Yu et al.*, 2004; *Le Goff and Gallet*, 2004; *Dekkers and Böhnel*, 2006; *Tarduno et al.*, 2006] have been proposed to improve this situation and to ultimately acquire a larger number of reliable field determinations (see *Valet* [2003] for the most recent review). In fact, the suitability of the results mostly depends on criteria that have been put forward by the different authors but frequently do not incorporate any thorough comparison with the modified Thellier-Thellier procedure or its direct derivatives such as the Coe or the recent "Triaxe" approach [*Le Goff and Gallet*, 2004].

[3] Absolute paleointensity determinations are an indirect way for quantifying past geomagnetic field strengths relying on thermomagnetic remanence (TRM) acquisition. As the TRM strength is not only a function of the applied field, but also depends on the magnetic properties of remanence carriers, the latter can have an influence on the result accuracy. Compared to baked archeological materials, lavas are generally less homogeneous and their paleointensity results are more scattered [e.g., *Donadini et al.*, 2007]. Ideally, different paleointensity determination methods should yield the same results, but this is sometimes not the case. For instance, *Yamamoto et al.* [2003] compared the conventional Coe-Thellier method with the Shaw LTD-DHT method [*Tsunakawa et al.*, 1997; *Tsunakawa and Yamamoto*, 1999] using historical lavas from 1960 Kilauea flow of Hawaii and found that the latter yields more correct results. As the investigated flow underwent low-temperature oxidation, a thermochemical remanence had formed and the conventional method failed, because it involves more intense heating

than the Shaw LTD-DHT method. While values obtained with the latter were in agreement with the definitive geomagnetic reference field (DGRF 1965), the conventional method overestimated the expected value by about 35%. *Hill and Shaw* [2000] studied two sections of the same flow, 16 m away from each other, with the microwave technique. While one of the two underestimated the expected field value by about 13%, the other yielded correct values. *Böhnel et al.* [2003] performed Thellier-Coe and microwave paleointensity analyses on a historical Mexican lava flow (330 A.D.) and found that the standard deviation is similar (~15%) for both methods, and that the average microwave paleointensity is about 13% lower than the Thellier-Coe average. They concluded from their study that the microwave technique yields a higher quality and success rate than the conventional method. In summary: beside magnetomineralogical variations within lava flows, which are responsible for scatter, discrepancies between different paleointensity determination techniques are likely, because different physical processes are involved for NRM demagnetization and TRM acquisition. As shown by *Hill and Shaw* [2000], during microwave application, lava samples are heated up to 160°C. This means that in addition to the microwave thermoremanence (T_MRM), a low-temperature TRM may be acquired at the same time.

[4] Despite abundant and rich archeological findings, very few paleomagnetic and archeomagnetic studies have been conducted at Santorini. They mostly addressed geological problems such as the emplacement temperatures of lithic clasts contained in pyroclastic flows [e.g., *Wright*, 1978; *Downey and Tarling*, 1984; *Tarling and Downey*, 1989; *McClelland and Druitt*, 1989]. Geomagnetic field directions of the Minoan eruption, dated at 1627–1600 B.C. [*Friedrich et al.*, 2006], were obtained from archeological material originating from the Akrotiri excavation and from volcanic material of the Thera formation (1st and 2nd explosive cycle) [*Downey and Tarling*, 1984; *Tarling and Downey*, 1989]. While inclinations derived from both types of material give consistent results, declinations vary by about 10° [cf. *Downey and Tarling*, 1984; *Tarling and Downey*, 1989]. A few directional data from the post-Minoan intracaldera volcano, called Nea Kameni, have been compiled by *De Marco* [2007] using the database of *Jonkers et al.* [2003] who found historical values of $D = 1.7°$, $I = 57.6°$ for the 1571 A.D. Mikri Kameni lavas, $D = -4.4°$, $I = 41.4°$ for the Georgios lavas of 1868 and $D = -5.7°$, $I = 57.3°$ for the Liatsikas lavas of 1950. The historical lava flows from Santorini can potentially provide new constrains to the Greek archeomagnetic data set which has recently been integrated in the construction of an archeointensity reference curve [*De Marco et al.*, 2008].

[5] The present study is aimed at comparing and testing the currently used techniques for absolute paleointensity on Santorini historical lava flows. The results should help to constrain the uncertainties inherent to the construction of the record of absolute paleointensity for the past centuries in the Greek area. The paleointensity experiments have been preceded by detailed rock magnetic techniques in order to evaluate the thermochemical alteration of the magnetic minerals and to assess the magnetic characteristics of the remanence carriers.

2. Geological Settings and Previous Studies

[6] Santorini is located in the south Aegean volcanic arc (Hellenic arc) at about 36°24′N and 25° 23′E. The investigated samples originate from the small Palea Kameni and Nea Kameni islets (Figure 1), both located within the intracaldera volcano rising 500 m above the caldera floor. The islands are situated on a seismic lineament, (Kameni line), which appears to be a deep rupture in the lithosphere, allowing the ascension of mantle magma [*Papazachos and Panagiotopoulos*, 1993]. After the end of the second explosive cycle, culminating with the Minoan explosion dated to 1627–1600 B.C. [*Friedrich et al.*, 2006], the volcanic activity continued. The 46–47 A.D. and 726 A.D. eruptions built up the Palea Kameni and subsequent eruptions (1570–1573 A.D., 1707–1711 A.D., 1866–1870 A.D., 1925–1928 A.D., 1939–1941 A.D., 1950 A.D.) formed Nea Kameni. The different lava flows can easily be distinguished in the field and are described by *Fytikas et al.* [1990]. The sample nomenclature (Table 1) is the same as in the work by *Druitt et al.* [1999]. The lava flows consist of large and small blocks. Except for crater walls (e.g., Mikri Kameni), it is unclear whether the cooling position of the block coincides with the present-day position. Vast oriented sampling has therefore not been attempted. Instead, three to seven large mostly nonoriented hand samples have been taken from each flow on both islands (Figure 1).

[7] The chemistry of the Kameni lavas is uniformly of dacitic nature [*Barton and Huijsmans*, 1986; *Conticelli et al.*, 1998; *Francalanci et al.*, 1998] with gabbroic and basaltic enclaves [*Barton and*

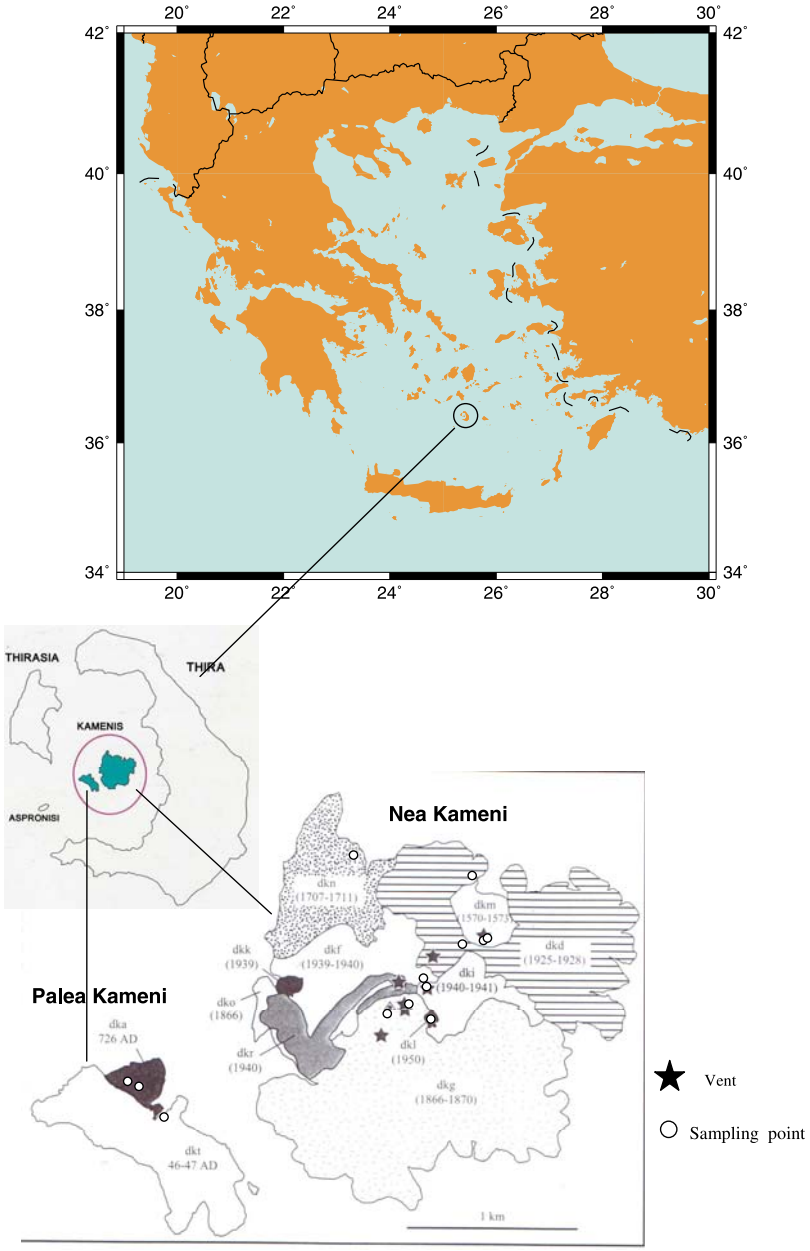

Figure 1. Geological map of Palea and Nea Kameni, redrawn from *Druitt et al.* [1999]. White circles represent sampling localities.

Huijsmans, 1986] and a porphyritic texture. The fine-grained groundmass is dominated by plagioclase microlites and phenocrysts of plagioclase (generally < 1 mm) and clinopyroxene phenocrysts (≤0.5 mm) with imbedded magnetite inclusions. Magnetite phenocrysts (<0.5 mm), with subhedral to anhedral grain forms [*Zellmer*, 1998] are also present. In contrast, microphenocrysts of magnetite have euhedral grain shapes [*Zellmer*, 1998], i.e., well-defined crystal forms. Magnetite phenocrysts and microphenocrysts are titaniferous with 14.0% to 16.4% per weight TiO_2 [*Barton and Huijsmans*, 1986] which corresponds to $Fe_{3-x}Ti_xO_4$ with x = 0.2–0.24 inferring Curie temperatures between 440°C and 470°C. There are major differences in color between the various lavas. Lavas from Nea Kameni island (compare Figure 1) are mainly black arising from a high content of volcanic glass resulting from fast cooling. Palea Kameni lavas, in particular lava dkt-46, are rather gray with a granular texture.

Table 1. Sample Code, Age, and Geochemical Composition of Lava Flows on Palea and Nea Kameni, Santorini[a]

Flow Code	Age	Name	*$Fe_2O_3^T$ (2σ = ±1.7%)	TiO_2 (2σ = ±2.5%)	Al_2O_3 (2σ = ±0.7%)	MgO (2σ = ±3.3%)	SiO_2 (2σ = ±0.5%)
dkt-46	46–47 A.D.	Thira (PK)	4.87	0.709	15.46	1.07	66.99
dka-726	726 A.D.	Agios Nikolaos (PK)	4.68	0.671	15.11	0.92	67.92
dkm-1570	1570–1573	Mikri Kameni (NK)	4.88	0.710	15.27	1.01	67.26
dkn-1707	1707–1711	Nea Kameni (NK)	5.08	0.741	15.38	1.10	66.77
dkg-1866	1866–1870	Georgios (NK)	5.47	0.776	15.49	1.28	65.95
dkd-1925	1925–1928	Dafni (NK)	5.68	0.786	15.60	1.40	65.38
dkf-1939	1939–1940	Fouqué (NK)	5.71	0.785	15.56	1.40	65.38
dkr-1940	1940	Reck and Smith (NK)	5.68	0.788	15.49	1.39	65.53
dki-1940	1940–1941	Niki lavas (NK)	5.32	0.745	15.59	1.28	65.92
dkl-1950	1950	Liatsikis lavas (NK)	5.86	0.798	15.57	1.54	65.04

[a]Geochemical data were obtained by *Zellmer* [1998] by X-ray fluorescence.

This indicates stronger mineral formation due to slower cooling rates.

3. Rock Magnetic Analyses

[8] Temperature dependence of induced magnetization was monitored by heating small pieces (not powder) of about 100 mg to 700°C with subsequent cooling at 100°C in a field of 800 mT. The experiment was performed using a variable field translation balance (VFTB). The high temperature dependence of low field susceptibility was analyzed for a few samples (small pieces, not powder) using a KLY-2 Kappabridge. The thermomagnetic measurements revealed the presence of two populations of magnetic minerals with two Curie temperatures (T_c). The first is associated with the dominant phase between 250°C and 320°C, while a minor phase has a T_c at about 500°C (Figure 2). The measurements further indicated excellent thermochemical stability below the upper Curie temperature for almost all samples (Figures 2b and 2d–2f). Titanomaghemite or ferrimagnetic iron sulfides can be excluded, due to the reversible thermomagnetic curves. If present, these minerals would transform into magnetite phases at higher temperatures, but there is no evidence that this happened during cooling from 600°C (compare Figures 2b and 2d–2f). The fact that thermomagnetic alteration is negligible and that the Curie temperature is below 580°C suggests that the magnetization is carried by substituted magnetites. Titanomagnetite appears to be the dominant ferrimagnetic mineral of both populations. One infers from their respective Curie temperatures (250°C to 320°C and 500°C) that TM52 to TM42 ($Fe_{2.48}Ti_{0.52}O_4$ to $Fe_{2.58}Ti_{0.42}O_4$) would be associated with the low-temperature phase, while TM15 ($Fe_{2.85}Ti_{0.15}O_4$) would be the carrier of the high-temperature phase [*Dunlop and Özdemir*, 1997]. Note that aluminum and/or magnesium impurities in the crystal lattice cannot be excluded. As mentioned in section 2, submillimeter sized magnetite phenocrysts and microphenocrysts were identified as TM20 to TM24, which correspond probably to our high Curie temperature phase. However, this phase plays only subordinate role as seen in Figure 2. The dominating magnetic mineral phase consists of magnetite inclusions which were observed by *Zellmer* [1998] in clinopyroxene phenocrysts and which we indentified now as titaniferous.

[9] The anisotropy of magnetic low field susceptibility has been studied for a set of 99 specimens. The degree of anisotropy (P') varies between 1.010 and 1.098, the mean being 1.050 and the shape parameter T ranges from −0.295 to 0.913, with a mean of 0.523. Only a few negative values were observed. The Kameni lavas show thus a low degree of anisotropy with mostly oblate ellipsoids.

Figure 2. (a–d) Typical examples of thermomagnetic curves measured in a field of 800 mT, without correcting paramagnetic contributions. The curves indicate low magnetic mineral alteration, except for specimens from flow dkt-46. The major magnetic mineral assemblages have Curie temperatures of about 300°C. Red and blue curves represent heating and cooling cycles, respectively. (e and f) Examples of high temperature dependence of magnetic susceptibility without paramagnetic correction. Colored curves represent successive heating cycles of the same specimen with different maximal temperatures. Darker and lighter colors represent heating curve and cooling curve, respectively. The black (heating) and gray (cooling) curves are from a different specimen of the same sample. The major ferrimagnetic phase has a Curie temperature of about 300°C and is resistant against heating to 500°C.

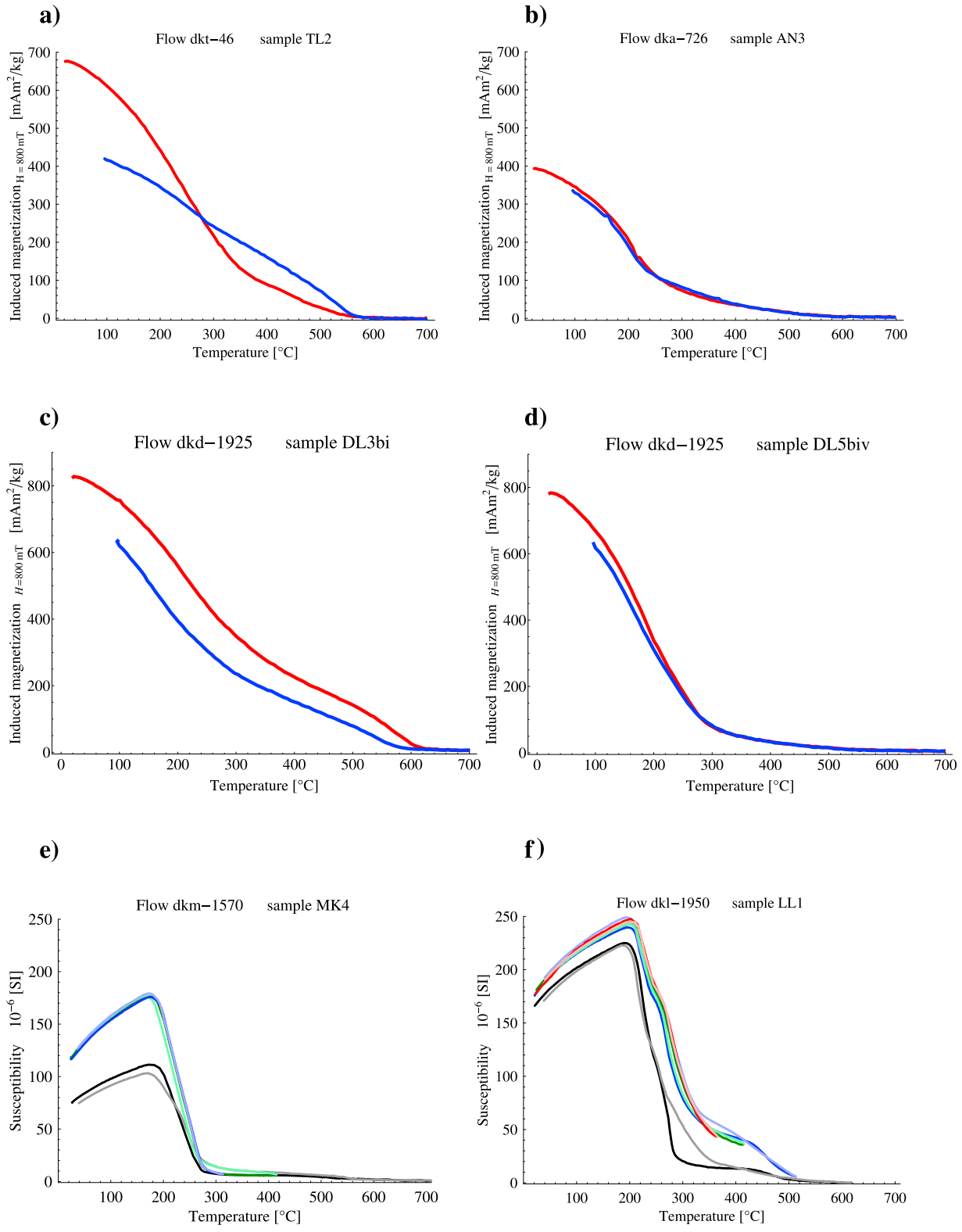
a)
Flow dkt−46 sample TL2
Induced magnetization H = 800 mT [mAm²/kg]
Temperature [°C]
b)
Flow dka−726 sample AN3
Induced magnetization H = 800 mT [mAm²/kg]
Temperature [°C]
c)
Flow dkd−1925 sample DL3bi
Induced magnetization H=800 mT [mAm²/kg]
Temperature [°C]
d)
Flow dkd−1925 sample DL5biv
Induced magnetization H=800 mT [mAm²/kg]
Temperature [°C]
e)
Flow dkm−1570 sample MK4
Susceptibility 10⁻⁶ [SI]
Temperature [°C]
f)
Flow dkl−1950 sample LL1
Susceptibility 10⁻⁶ [SI]
Temperature [°C]

Figure 2

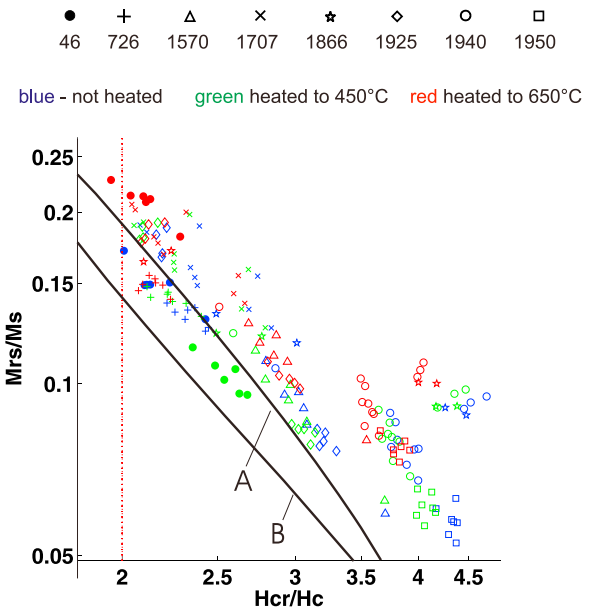

Figure 3. Bilogarithmic Day plot [*Day et al.*, 1977] of nonheated specimens (blue symbols) and after heating to 450°C (green symbols) and 650°C (red symbols) for different lava flows. As expected on a log-log scale, all the data plot more or less along a straight line inside the PSD range (red pointed line, boundary as given by *Dunlop* [2002]). Flows dka-726 (pluses), dkm-1570 (triangles), and dkl-1950 (squares) group rather well together, while the other flows show a distinct dispersion. Heating to 450°C does not considerably change H_{cr}/H_c and M_{rs}/M_s, except for flow dkt-46. Note that the date 1940 refers here to the three different lava flows that had formed between 1939 and 1941. Detailed measurements for each of these three flows can be found in Data Set S1. Lines A and B are the theoretical SD-MD mixing curves from *Dunlop* [2002] using coarse- and fine-grained magnetite end-members, respectively.

[10] Isothermal magnetization curves were measured in a "rotation" magnetometer [*Burov et al.*, 1986; *Jasonov et al.*, 1998], which consists of a rotating nonmagnetic disk spinning with a frequency of 15 Hz and which passes the sample to be measured through two induction coils during each turn. One of them is placed inside the pole tips of an electromagnet to measure induced magnetization, while remanence is measured a three-fourth turn later in the second induction coil housed in a μ-metal shield. After completing a full turn, the next field step is applied. The duration of magnetization at each field step is in the order of tenths of a second. This allowed us to scrutinize the evolution of characteristic parameters such as the acquisition curves of isothermal remanent magnetization (IRM), backfield curves, hysteresis loops with their descending branch and short-term remanence decay curves. Remanent and induced magnetization were measured at each field increment (~0.5 mT). Each specimen was measured three times to evaluate the experimental error. The bilogarithmic Day plot in Figure 3 gives a general overview of the hysteresis parameters. As expected on a log-log scale, the values of H_{cr}/H_c and M_{rs}/M_s plot along a straight line which falls within the pseudo single domain range of the Day plot. Flows dka-726, dkm-1570 and dkl-1950 group fairly together, while the others show a distinct dispersion. This indicates that there are not only magnetomineralogical differences between the flows but also inhomogeneities within certain flows. Particularly, flow dkd-1925 can be subdivided in two distinct populations (see diamond symbols in Figure 3).

[11] When comparing the Day plot with the mixing model of *Dunlop* [2002], one notices that our data neither plot really well along the magnetite or titanomagnetite SD-MD mixing line, nor follow the titanomagnetite grain size trend of *Day et al.* [1977] synthetic titanomagnetites. However, they are in fair agreement with the grain size dependence described by *Hartstra* [1982] for natural, optically homogeneous titanomagnetite (14.62% TiO_2) containing submicroscopic iron-rich inclusions. Apparently, there are grain size variations between and inside the different lava flows (particularly for flow dkd-1925, see Table 2), as already suggested by the different coloration. Flows dkt-46, dka-726 and dkn-1707 contain rather fine grained titanomagnetite than flows dki-1940 and dkl-1950.

[12] *Hartstra* [1982] investigated also the grain size dependence of titanomagnetite with distinct exsolution lamellae showing that exsolution considerably reduces the grain size dependence in the Day plot. We argue that exsolution is less common in our samples, because our data span the whole PSD field, which is not the case for *Hartstra*'s [1982] samples exhibiting exsolution lamellae.

[13] Short-term decay of isothermal remanence (IRM loss) was monitored with the aforementioned rotation magnetometer in order to test whether superparamagnetic grains or grains in the vicinity of the SP/SD boundary (which might be formed during postcooling weathering) are present in the samples. Most Kameni dacites do not contain considerable amounts of such grains. On the average, about 2 percent of IRM_{-500mT} is lost within 100 s (Table 2). For comparison we measured the Tiva Canyon tuff *TC04*, with a volume distribution covering the SP/

Table 2. Bulk Rock Magnetic Parameters of Single Specimens From Different Lava Flows on Palea and Nea Kameni[a]

	$IRM_{500\ mT}$ (mAm^2/kg)	H_{cr}[b] (mT)	Interaction Parameter $R(H_{cr})$	IRM Loss in 100 s (%)	H_{cr}/H_c	M_{rs}/M_s[c]	High Field Susceptibility (400; 500 mT) (10^{-8} m^3/kg)
			dkt-46: N = 4, n = 6				
Mean	96	26.4	0.33	0.7	2.2	0.150	1.9
Stdev	5	1.3	0.04	0.1	0.1	0.013	0.2
Stdev %	6	4.9	10.97	18.1	6.4	8.433	11.1
			dka-726: N = 3, n = 7				
Mean	66	18.4	0.35	1.5	2.3	0.131	2.4
Stdev	5	0.9	0.02	0.4	0.1	0.007	0.2
Stdev %	8	4.9	6.66	26.4	4.2	5.250	9.0
			dkm-1570: N = 4, n = 6				
Mean	59	15.5	0.40	1.1	3.0	0.097	2.5
Stdev	9	1.0	0.04	0.3	0.5	0.023	0.1
Stdev %	15	6.8	11.07	27.6	16.3	24.187	3.9
			dkn-1707: N = 4, n = 9				
Mean	110	24.0	0.41	2.0	2.4	0.160	2.9
Stdev	45	7.4	0.03	0.8	0.3	0.025	0.4
Stdev %	41	31.0	8.24	37.6	11.2	15.625	13.1
			dkg-1866: N = 2, n = 4				
Mean	95	29.8	0.38	1.7	3.6	0.108	2.8
Stdev	26	2.6	0.04	0.9	1.0	0.021	0.3
Stdev %	28	8.7	10.08	53.4	27.3	19.177	10.5
			dkd-1925: N = 4, n = 9				
Mean	96	23.4	0.41	2.1	2.8	0.123	2.5
Stdev	53	10.9	0.02	0.4	0.5	0.052	0.2
Stdev %	55	46.4	5.17	17.5	19.5	41.935	9.7
			1939–1941[d]*: N = 8, n = 12*				
Mean	77	23.0	0.41	2.8	4.0	0.085	3.1
Stdev	10	4.9	0.05	1.5	0.5	0.011	0.2
Stdev %	14	21.4	12.15	53.0	12.1	12.790	6.0
			dkl-1950: N = 3, n = 7				
Mean	45	15.8	0.40	1.6	4.3	0.057	2.7
Stdev	3	1.1	0.03	0.2	0.1	0.005	0.2
Stdev %	7	6.7	7.84	15.7	1.3	8.539	5.9

Material for Comparison	Specimen	Domain State	$IRM_{500\ mT}$ (mAm^2/kg)	H_{cr} (mT)	$R(H_{cr})$	IRM Loss (%)	H_{cr}/H_c	M_{rs}/M_s	χ_{HF} (10^{-8} m^3/kg)
Ferrofluid (fixed)	FF607	SP+SD?	3	15.5	0.45	37.1	6.5	0.050	−0.1
Tiva Canyon TC04M	030	SP+SSD	13	27.2	0.40	11.3	18.1	0.046	0.0
Magnetic tape	3M	SD	240	42.5	0.30	1.0	1.5	0.300	−0.8
Tiva Canyon TC05_9.0	114	SD	88	50.1	0.44	1.9	1.7	0.290	0.0
Baked clay(black)	BY000.rt	SD	331	77.2	0.47	1.5	1.6	0.390	2.1
Wright magnetite	W112982	MD	1778	23.3	0.31	0.6	7.7	0.020	−33.2

[a]*N* is the number of studied samples per flow, and *n* is the total number of specimens per flow studied for rock magnetic properties. The magnetostatic interaction parameter $R(H_{cr})$ was calculated from backfield curves and IRM acquisition curves [see *Fabian and von Dobeneck*, 1997, equations 20, 21, and 26]. See Data Set S1 in the auxiliary material for individual measurements. SP, superparamagnetic; SSD, stable single-domain; SD, single-domain; MD, multidomain; Stdev, standard deviation.

[b]Obtained from remanent backfield curves.

[c]Referring to a maximum magnetizing field of 500 mT.

[d]Note that for the three studied lavas erupting between 1939 and 1941 no distinction was made here. Details are given in Data Set S1.

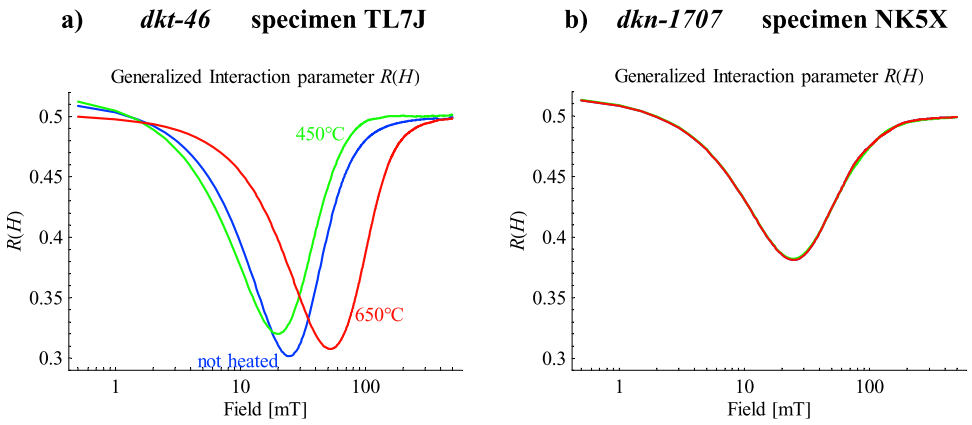

Figure 4. Generalized magnetostatic interaction parameter $R(H)$ as proposed by *Fabian and von Dobeneck* [1997] in function of the magnetizing field H before (blue) and after heating to 450°C (green) and 650°C (red). The curves for specimen TL7J are different due to thermochemically induced changes of the remanent coercive force spectrum (compare Figure 5). Heating, however, has no substantial influence on the degree of magnetostatic interaction.

stable SD boundary [*Jackson et al.*, 2004]. It loses about 11% of IRM_{500mT} within 100 s (Table 2).

[14] All curves related to high field experiments (hysteresis loops, backfield curves and IRM acquisition) were separated into elemental magnetization curves [*Fabian and von Dobeneck*, 1997]. This allowed more detailed rock magnetic interpretations such as for instance the generalized magnetostatic interaction parameter $R(H) = \frac{IRM(H) - SIRM_{AF}(H)}{2M_{rs}}$, with $IRM(H)$ being the isothermal remanence acquisition curve, $SIRM_{AF}(H)$ the alternating field demagnetization curve of isothermal saturation remanence and M_{rs} the saturation remanence. $SIRM_{AF}(H)$ has not been directly measured but was substituted by the sum of $IRM(H)$ and the backfield curve, $BF(H)$, as suggested by *Fabian and von Dobeneck* [1997]. $R(H)$ indicates magnetostatic interactions between single domain grains as well as domain interaction in multidomain grains. According to *Fabian and von Dobeneck* [1997], the *Cisowski* [1981] interaction parameter (R) is related to irreversible energy losses of remanence contributions due to the action of the demagnetizing field at $H = H_{cr}$. The interaction parameter of most samples shows a minimum at about 0.4 that is slightly below H_{cr}, indicating a small degree of magnetostatic interaction, like as for most natural materials (material for comparison in Table 2). The smallest R value 0.33 ± 0.04 was found in flow dkt-46. Furthermore, heating experiments showed that the interaction degree is not influenced by heating (see example in Figure 4).

[15] In order to document thermochemical alterations during multiple heatings and coolings that are required by standard paleointensity techniques, small cuboidal specimens (~6 × 8 × 23 mm) were cut from hand samples and heated for about half an hour in air before being cooled in zero field using a Schonsted thermal demagnetizer. The experiment was conducted at 150°C, 250°C, 350°C, 450°C, 550°C and 650°C. After each step, isothermal magnetization curves were measured with the rotation magnetometer. Remanent backfield curves were filtered before calculating their derivative (coercive force spectrum) using the MAGMIX software [*Egli*, 2003a, 2003b].

[16] Heating influenced the hysteresis properties to a minor extent, only. In general, H_{cr}/H_c was lowered with increasing temperature while the M_{rs}/M_s ratio increased (green and red colors in Figure 3). The differences in the coercivity spectrum before and after heating at temperature T_i were quantified using the following parameter [cf. *Spassov and Hus*, 2006]:

$$\delta_{BF_{\Delta(T_i-T_{23^\circ C})}}(T_i) = \frac{\int_{H_{min}}^{H_{max}} \sqrt{(f_{T_i}(H) - f_{23^\circ C}(H))^2}\,dH}{\int_{H_{min}}^{H_{max}} f_{23^\circ C}(H)\,dH} \cdot 100\% \quad (1)$$

where $f_{23°C}(H)$ is the coercive force spectrum of the unheated sample, $f_{T_i}(H)$ the one measured after heating to temperature T_i and H is the magnetizing field. This approach was applied to the coercivity spectra of the remanence derived from remanent backfield curves (Figure 5). The gray line in Figures 5b and 5d represents the root of the squared difference between the spectra of remanent coercive force prior and after heating, and indicates that heating affected the intermediate coercivities. Only the specimen from flow dkt-46 exhibited a strong

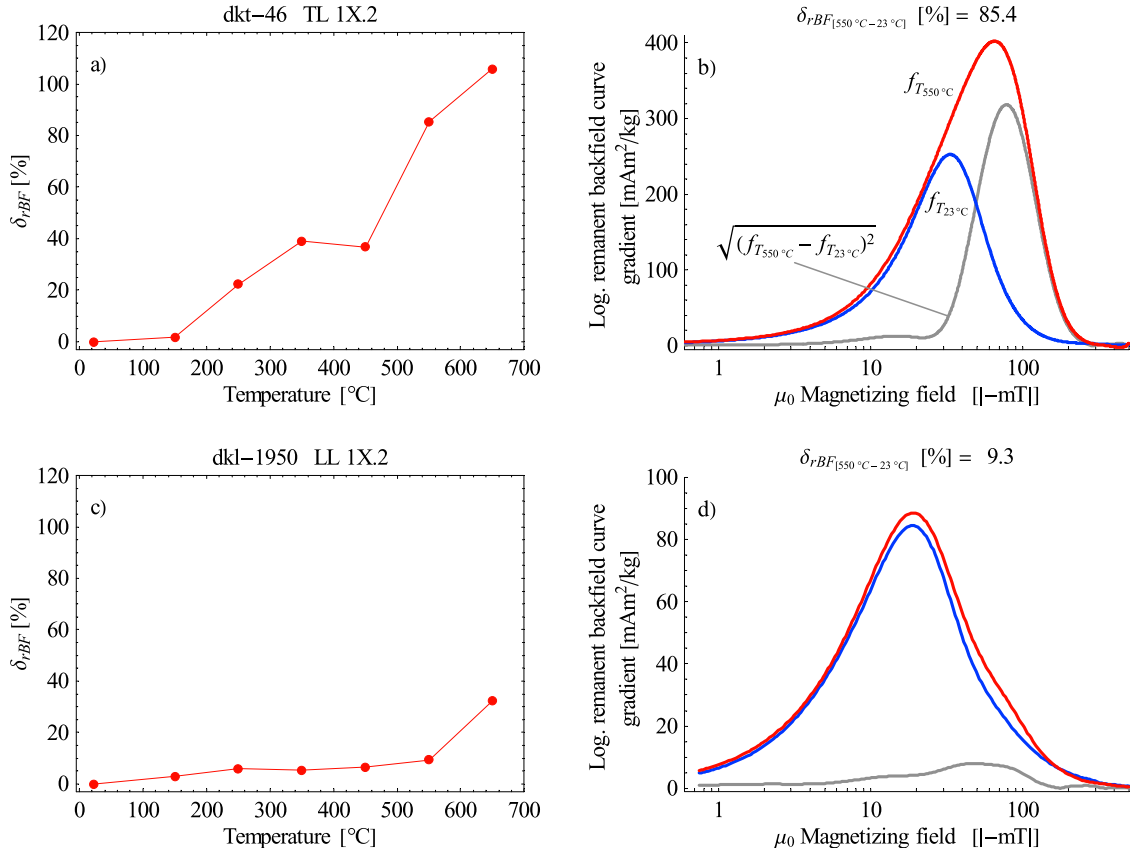

Figure 5. (a and c) Percentage of coercivity spectral change (see equation (1)) for different successive heating steps. (b and d) Example of estimating the spectral change for temperature step 550°C. Remanent coercivity spectrum obtained from backfield curves, before $f_{T_{23°C}}$ (blue) and after exposure to high temperatures $f_{T_{550°C}}$ (red). The gray curve is the squared difference between both spectra ($\sqrt{(f_{T_{550°C}} - f_{T_{23°C}})^2}$). Heating above 550°C causes a neoformation of grains with intermediate coercive forces. The numbers given on top of the graphs represent the percentage of change of the whole coercivity spectrum after heating to 550°C with respect to the spectrum of the nonheated sample (compare equation (2)). Only flow dkt-46 shows considerable neoformation of remanence carriers upon heating. All other flows show a behavior such as in Figures 5c and 5d.

alteration of its magnetic minerals (Figures 5a and 5b), while those from all other flows remained very resistant after being heated to 450°C (e.g., Figures 5c and 5d).

4. Paleointensity Determination

[17] A prerequisite for paleointensity experiments is the absence of thermochemical alterations. Most samples did not show significant alteration below their Curie temperature except flow dkt-46. Therefore, this flow was a priori excluded from paleointensity determination.

4.1. Modified Thellier Experiments

[18] Two kinds of experiments have been processed using a modified Thellier-Thellier protocol [*Thellier and Thellier*, 1959]. In the first case 18 paleomagnetic standard sized cylindrical specimens were heated in a Schonstedt thermal demagnetizer in zero field for about 45 min and subsequently cooled in a nominal field of 40 μT. Field mapping in the cooling chamber of the demagnetizer revealed variable deviations up to 10 μT in amplitude from the nominal value. The specimens were therefore always heated at the same position within the oven during the entire experiment, and the corresponding applied field at each position was taken for paleointensity calculation. The majority of the specimens was heated at 18 double steps between 100°C and 520°C. To those we added 9 checks of partial thermoremanent magnetization (pTRM). Remanence measurements were performed using an upgraded three-axis 2G Enterprises cryogenic magnetometer with DC SQUIDS and a sample

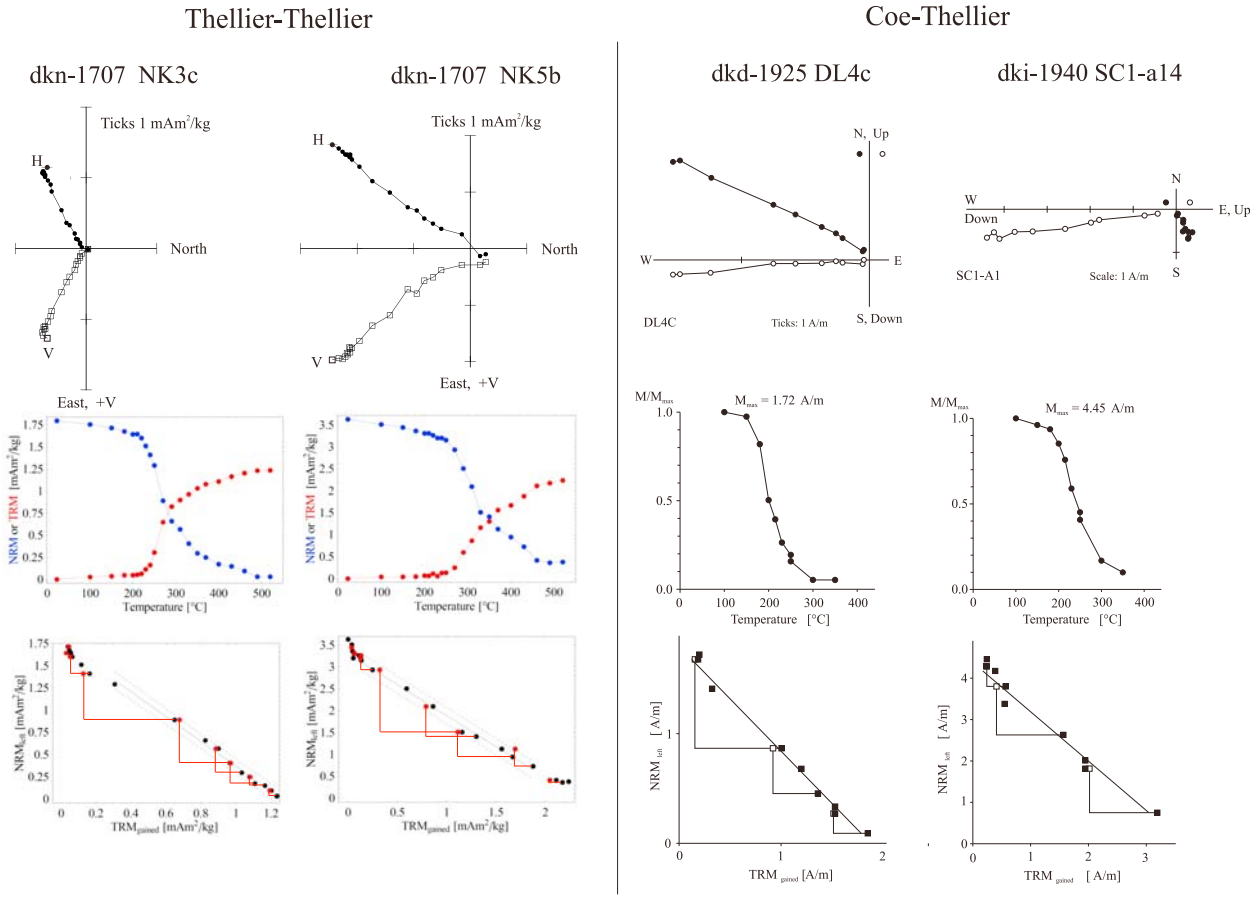

Figure 6. Examples of successful paleointensity determinations with (left) the Thellier-Thellier method and (right) the Coe-Thellier method. (top) The Zijderveld diagrams show a stable single directional component, secondary components are absent. (middle) The NRM unblocks over a rather narrow temperature interval of about 100°C. (bottom) The corresponding Arai diagrams including the fitted slope. The dashed lines are the 95% confidence envelope of the mean slope for single observations. Note that thermochemical alteration is almost absent and the pTRM checks (red filled dots or empty squares) fall into the error envelope of the slope. The pTRM checks are considered as positive if mean pTRM deviation (see section 4.1 for explanation) of the fitting interval is below 5.5%.

access of 7.6 cm at the paleomagnetic laboratory of the Centre de Physique du Globe Dourbes in Belgium. being equipped with a Cryomech 4 K (model PT405) pulse tube cryorefrigerator without liquid helium reservoir.

[19] The Coe version [*Coe*, 1967] of the Thellier-Thellier experiment was applied to 24 specimens but with a small change in the protocol. Instead of measuring the NRM first, we preferred to apply a TRM before heating the sample in zero field [*Aitken et al.*, 1988; *Valet et al.*, 1998; *Herrero-Bervera and Valet*, 2005]. Each heating step beyond 280°C was accompanied either by a pTRM check or a second measurement of the residual NRM. The TRMs were performed in presence of a 30 μT field. For the Coe version paleointensity determination procedure, we used a Pyrox oven with a temperature gradient not larger than 0.5°C/cm. Heating was controlled by three external thermocouples, and temperature was accurately monitored by three other thermocouples located close to the samples in a Pyrox oven. The samples were heated for at least 1 h depending on the temperature step. Cooling was accelerated by cool pulsed air and lasted between 20 and 30 min. The measurements were processed in the shielded room of Paris, Institut de Physique de Globe using a JR-5 fluxgate magnetometer. The temperature steps (usually by increments of 50°C) have been defined according to the evolution of the NRM during demagnetization. The PaleoMac software [*Cogné*, 2003] was very helpful for data processing.

[20] A few examples of both sets of experiments have been combined in Figure 6 which shows the demagnetization diagrams, the evolution of NRM intensity during demagnetization and the Arai plots of successful paleointensity determinations. A dominant characteristic is that the TRM and the NRM of these samples block and unblock, respectively, within a narrow range of temperature of about 100°C, while the absence of alteration is reflected by the pTRM checks which fall very close to the error envelope of the NRM/TRM slope.

[21] The quality of the data was defined following several criteria. We only considered demagnetization diagrams with a well defined characteristic segment decreasing toward the origin. The additivity of partial TRMs and independence of pTRMs requires equal blocking and unblocking temperatures. These are best fulfilled by an assemblage of noninteracting single-domain grains with nonoverlapping blocking temperature intervals and unimodal grain size distribution [*Dunlop and Özdemir*, 1997]. Like for 99% of the natural basaltic samples, the dacitic lava samples from Palea and Nea Kameni show pseudo-single-domain rather than single-domain behavior, which can generate small differences between the unblocking and blocking temperature spectra. For these reasons and in accordance with recent studies from contemporaneous Hawaiian flows [*Herrero-Bervera and Valet*, 2009], another requirement was that the NRM-TRM plots displayed a linear trend over the temperature spectrum associated with the decay of the NRM and that the remanence was carried by a unique magnetic phase with a narrow unblocking temperature spectrum. A direct consequence of this criterion is that samples with an *f* quality parameter (defined as the fraction of remanence involved in the paleointensity calculation) lower than 50% have been rejected (selection criterion 1). The samples that failed to show a well defined linear distribution of the NRM-TRM points were discarded. The last selection relied on the deviations of the pTRM checks from the initial pTRM. *Selkin and Tauxe* [2000] proposed to normalize this difference between the two successive pTRMs performed at the same temperature with respect to the length of the selected NRM-pTRM segment and expressed it as a percentage (DRAT). Since the NRM is not involved in the deviations of the pTRM checks, we preferred to simply normalize with respect to the TRM segment used for the paleointensity calculation and the mean value of all deviations was referred as the mean "pTRM deviation." For the same reason we cannot refer to the CDRAT defined by *Kissel and Laj* [2004] but rejected samples with one pTRM check characterized by a large deviation while other ones would be acceptable. Following previous discussion on the subject and investigations carried out for recent lava flows from Hawaii [*Herrero-Bervera and Valet*, 2009], it is reasonable to consider that the upper limit of the mean pTRM deviation should not go far beyond 5.5% (selection criterion 2). Table 3 summarizes the evolution of the successive steps for each lava flow. About 75% of the samples displayed linear NRM-TRM diagrams but only 50% had acceptable pTRM deviations. The largest success rate (100%) was obtained for flow 1941. Note that this success rate is quite high with respect to most studies which usually do not exceed 15%–20%. It results from the magnetic homogeneity of the samples. Indeed, it is noticeable that all samples which provided successful determinations are characterized by a unique phase of titanomagnetite with a very narrow range of grain sizes derived from a narrow unblocking temperature spectrum. These observations are consistent with recent observations derived from a study of the 1955 and 1960 Hawaiian flows [*Herrero-Bervera and Valet*, 2009].

4.2. Microwave Experiments

[22] The 14 GHz microwave system of the University of Liverpool was used to conduct microwave experiments on a large set of 98 specimens. The NRM of small cylindrical specimens (5 mm diameter, 3 mm length) was measured and gradually replaced by a microwave "thermoremanent" magnetization (T_MRM) which was induced by an ambient field perpendicular to the characteristic remanent magnetization (ChRM) direction (perpendicular field paleointensity method) [*Kono and Ueno*, 1977; *Hill and Shaw*, 1999]. High-frequency microwaves directly excite the spin system so that there is no need to heat the bulk sample to generate phonons [*Walton et al.*, 1992, 1993; *Hill and Shaw*, 2000]. The Liverpool 14 GHz system incorporates a resonant microwave cavity and a SQUID cryogenic magnetometer. This method only requires one microwave application for each power step. The microwaves have been applied for a maximum duration of 10 s with microwave power being increased stepwise as for increasing temperature settings in a thermal demagnetizer [*Hill and Shaw*, 1999]. After preliminary tests, the strength of the DC field was adjusted to approximate the expected

Table 3. Paleointensity Mean Values for Each Lava Flow, Specified for Each Determination Technique[a]

	Mean Values of Different Paleointensity Determination Techniques											
	Thellier			Microwave			Shaw			Triaxe		
Year	N_1/T	N_2/T	H_{Pal} (μT) ± SD (μT)	N_1/T	N_2/T	H_{Pal} (μT) ± SD (μT)	N_1/T	N_2/T	H_{Pal} (μT) ± SD (μT)	N_1/T	N_2/T	H_{Pal} (μT) ± SD (μT)
46	0/0	0/0	–	0/5	0/5	–	0/0	0/0	–	–	0/0	–
726	6/8	5/8	48.3 ± 2.7	10/16	5/16	48.2 ± 7.5	3/3	0/3	–	–	1/2	50.4
1570	2/5	2/5	43.9 ± 2.8	7/8	3/8	28.2 ± 6.3	3/3	0/3	–	–	0/2	–
1707	5/7	4/7	42.4 ± 1.6	9/13	5/13	44.9 ± 5.8	3/3	1/3	40.8	–	1/1	40.6
1866	1/2	0/2	–	3/4	1/4	40.9	0/0	0/0	–	–	1/3	42.1
1925	4/6	3/6	41.6 ± 8.4	12/22	8/22	46.3 ± 10.1	0/0	0/0	–	–	0/1	–
1940	5/5	3/5	43.1 ± 1.6	5/17	3/17	31.2 ± 1.6	0/0	0/0	–	–	1/4	36.3
1941	5/5	5/5	42.9 ± 2.8	3/4	3/4	37.5 ± 1.4	0/0	0/0	–	–	2/3	40.5 ± 2.2
1950	3/4	1/4	41.7	6/9	4/9	32.0 ± 9.3	0/0	0/0	–	–	3/5	35.5 ± 1.4

[a] N_1/T represents the number of successful determinations with respect to the total number T of specimens measured using selection criterion 1 (quality parameter $f > 50\%$, see section 4.1), and N_2/T is the same as N_1/T but after applying the selection criterion 2 (mean pTRM deviation < 5.5%, see section 4.1). SD is the standard deviation for single observations. Note that flow dkf-1939 had formed between November 1939 and July 1940, flow dkr-1940 formed in July 1940, and flow dki-1940 formed between November 1940 and July 1941. We thus assigned them to the years 1940, 1940, and 1941, respectively.

paleointensity following the recommendations of *Tanaka and Kono* [1984].

[23] During the perpendicular field paleointensity method the magnetizing field is applied in the plane of the ChRM, the inclination being 0° and the declination 90° away from that of the ChRM. The latter was isolated by initial microwave demagnetization at low power. Two angles were defined: φ_1 = angle between measured total remanence (i.e., partial T_MRM + residual ChRM) and the residual ChRM; φ_2 = angle between measured total remanence and applied field. Our criterion is that only those samples were accepted whose sum of φ_1 and φ_2 did not exceed 90° ± 0.5°. The perpendicular field method, of course, assumes that the T_MRM is acquired parallel to the magnetizing field which holds true for samples with negligible TRM anisotropy (ATRM). Our anisotropy of susceptibility data, which may be considered as first-order indicator of the ATRM, give no indication of strong anisotropy, as discussed before.

[24] The vertical component of the NRM direction showed a single stable component behavior (Figures 7a–7d). As described before, all secondary components with low unblocking power have been demagnetized before the paleointensity determination. The NRM unblocking range is much broader (Figures 7e–7h) than in the Thellier experiments (compare Figure 6, middle). This comparison demonstrates that different generation of demagnetizing energy, i.e., thermal for Thellier and dielectric for microwave, and its absorption by the sample does not affect exactly the same unblocking populations.

[25] In order to disqualify unsuccessful paleointensity determinations we have applied the same selection criteria as for the Thellier methods. Like for standard paleointensity experiments we have plotted the NRM remaining against TRM acquisition (Figures 7i–7l) and we used the same parameters *f*, *g*, *q* [*Coe et al.*, 1978]. Thirty three percent of the samples were selected for the calculation of paleointensity. This relatively low success rate may result from low-temperature transformations that are likely to occur in samples with low Curie temperatures, as mentioned above.

4.3. Experiments Using the "Shaw" Technique

[26] The protocol described by *Shaw* [1974] using alternating magnetic fields (AF) was applied to a small set of 9 specimens. Stepwise NRM and TRM

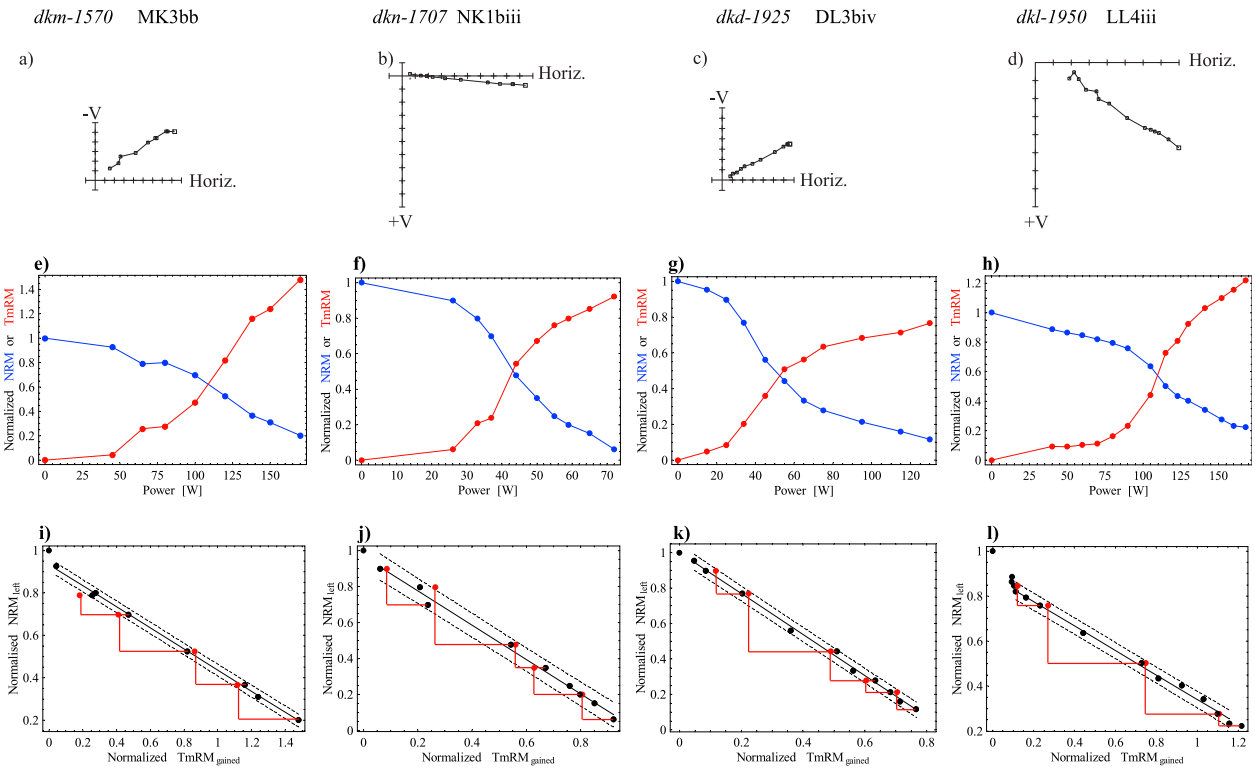

Figure 7. Examples of successful microwave paleointensity determination for specimens from four different flows. (a–d) Directional stability of the vertical NRM component during the paleointensity experiment. As the field is applied in the horizontal plane 90° away from that of the ChRM, only ChRM changes in the vertical plane could be observed. The direction is stable; however, the presence of viscous overprints cannot be tested because the perpendicular method requires a single directional NRM component and the sample was therefore demagnetized with microwave powers between 0 and the first step used for paleointensity determination. (e–h) NRM demagnetization (blue) and TRM acquisition (red) normalized to their corresponding maximal values. (i–l) Arai plots of the concerned specimens. The dashed lines are the 95% confidence envelope of the mean slope (black solid) for single observations. The pT_MRM checks are considered as positive if mean pT_MRM deviation (see section 4.1 for explanation) of the fitting interval is below 5.5%.

demagnetization were performed up to maximal AF peak field of 105 mT using the in-line alternating field demagnetizer and automated sample handling system of the 2G cryogenic magnetometer. A uniaxial TRM was acquired during 45 min in field cooling (H_{lab} = 40.4 μT) from 450°C or 550°C using a Schonsted thermal demagnetizer with a direct current (DC) coil. Before and after TRM acquisition a uniaxial anhysteretic remanent magnetization (ARM) was imparted using a 40 μT

Figure 8. Examples of paleointensity determinations based on AF demagnetization curves as proposed by *Shaw* [1974]. (a–d) Not accepted specimen and (e–h) accepted specimen. Figures 8a and 8e show the alternating field demagnetization curves of NRM (blue), TRM (red), $ARM_{before\ heating}$ (cyan), and $ARM_{after\ heating}$ (magenta). Equal area and Zijderveld diagrams (Figures 8b and 8f) reveal stable directions during NRM demagnetization. A viscous component which is demagnetized at 20 mT is particularly present in flow dka-726 (Figure 8b) and probably responsible for paleointensity overestimation (compare Table 3). The fitting interval was chosen on the degree of linearity of Figures 8c and 8g, showing the relation between NRM and $ARM_{before\ heating}$ (blue) and between TRM and $ARM_{after\ heating}$ to 450°C (red). Figures 8d and 8h show the *NRM TRM*$_{corr}$ regression line from which the paleointensity F_a was determined. *TRM*$_{corr}$ is the corrected TRM as proposed by *Rolph and Shaw* [1985]. Green points were taken into account for the regression. The black dashed lines represent the error of the mean slope (black line) for single observations with a confidence limit of 95%.

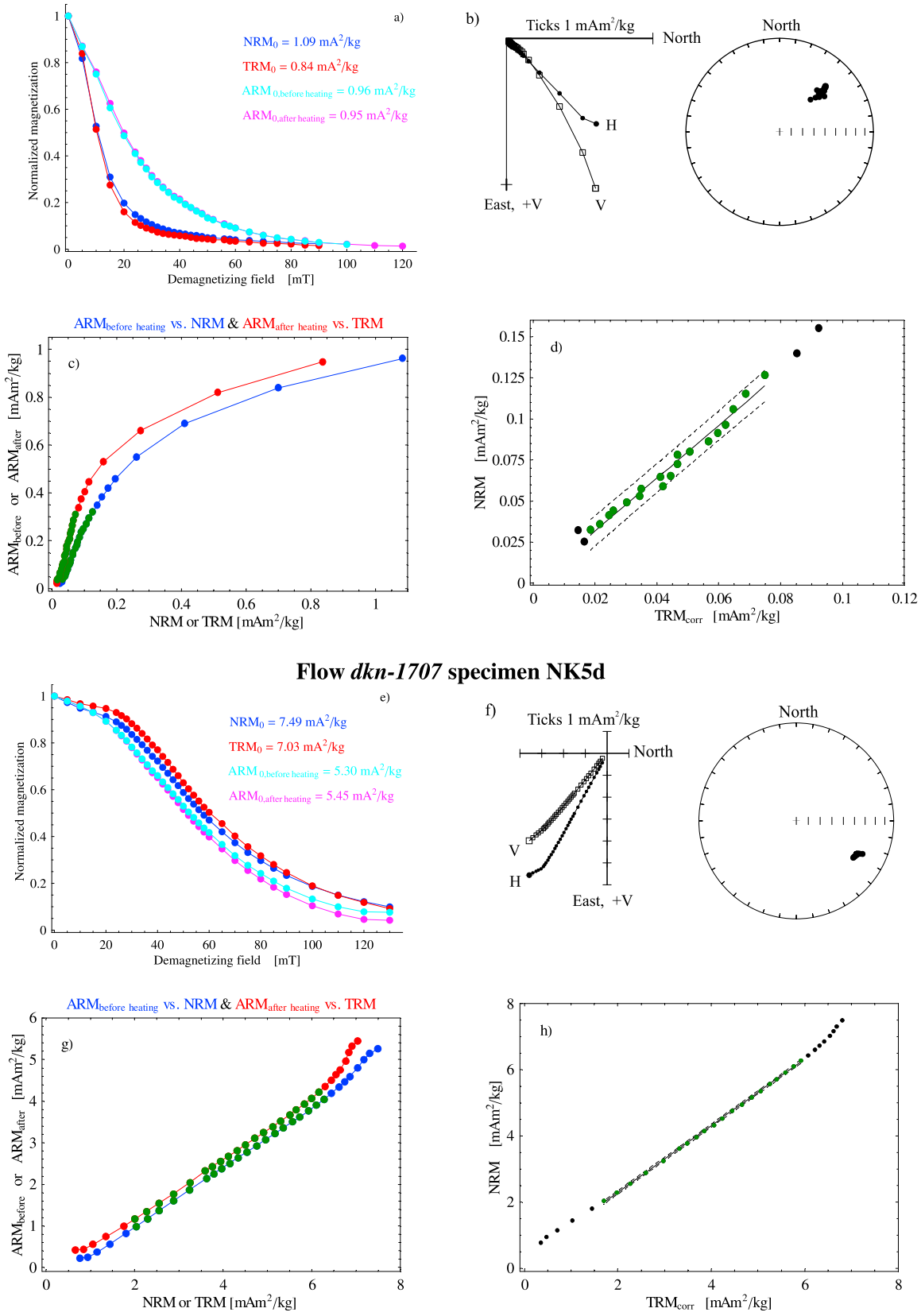
Flow dka-726 specimen AN5.1b
a)
NRM0 = 1.09 mA2/kg
TRM0 = 0.84 mA2/kg
ARM 0,before heating = 0.96 mA2/kg
ARM0,after heating = 0.95 mA2/kg
Normalized magnetization
Demagnetizing field [mT]
b)
Ticks 1 mAm2/kg
North
H
East, +V
V
North
ARMbefore heating vs. NRM & ARMafter heating vs. TRM
c)
ARMbefore or ARMafter [mAm2/kg]
NRM or TRM [mAm2/kg]
d)
NRM [mAm2/kg]
TRMcorr [mAm2/kg]
Flow dkn-1707 specimen NK5d
e)
NRM0 = 7.49 mA2/kg
TRM0 = 7.03 mA2/kg
ARM 0,before heating = 5.30 mA2/kg
ARM0,after heating = 5.45 mA2/kg
Normalized magnetization
Demagnetizing field [mT]
f)
Ticks 1 mAm2/kg
North
V
H
East, +V
North
ARMbefore heating vs. NRM & ARMafter heating vs. TRM
g)
ARMbefore or ARMafter [mAm2/kg]
NRM or TRM [mAm2/kg]
h)
NRM [mAm2/kg]
TRMcorr [mAm2/kg]

Figure 8

direct field and a peak alternating field of 105 mT and followed by demagnetization at the same steps as for the NRM and the TRM. In order to account for possible thermochemical changes in the magnetic mineral content, we applied the correction formula proposed by *Rolph and Shaw* [1985]:

$$TRM_{corr}(H) = TRM(H) \cdot \frac{ARM_1(H)}{ARM_2(H)} \quad (2)$$

As ARM and TRM were acquired along one axis, only the remanence component along this axis was used for data analysis and interpretation. Result quality was assessed in the same manner as for Thellier methods.

[27] Paleointensity determinations obtained by the *Shaw* [1974] alternating field demagnetization method are presented in Figure 8. A viscous directional component is demagnetized at about 20 mT (Figures 8b and 8f). The correlation of NRM and TRM demagnetization was frequently limited over a small part of the remanent coercive force spectrum which resulted into low f and q values. Two selection criteria were established: 1. Only samples with a linear $ARM_{\text{before heating}}$ NRM and $ARM_{\text{after heating}}$ TRM were retained. 2. Only samples with and NRM fraction greater than 50% and showing differences smaller than 5% between NRM-TRM and $ARM_{\text{before heating}}$-$ARM_{\text{after heating}}$ demagnetization curves were finally accepted. This parameter was calculated as follows:

$$\Delta_{NRM,TRM} = \frac{\sqrt{\frac{\sum_{i=1}^{n} NRM(H_i) - TRM(H_i)}{n}}}{NRM_{H=0}} \quad (3)$$

where $NRM(H_i)$ and $TRM(H_i)$ are the AF demagnetization curves of natural and thermal remanence, respectively, n is the number of points used for paleointensity determination and $NRM_{H=0}$ is the initial NRM.

[28] Three flows were studied with three specimens each. After selection, only one specimen remained from flow dkn-1707 with a final paleointensity in agreement with the Thellier techniques. In general, the high failure rate is probably not due to thermochemical alteration during the laboratory TRM acquisition, because the average difference between $ARM_{\text{before heating}}$-$ARM_{\text{after heating}}$ is only 3.2% for all nine studied specimens. We argue instead that differences between NRM and TRM intensity may be responsible. Concerning the non accepted specimen from flow dka-726 (Figure 8a), the initial TRM_0 is about 23% smaller than the NRM_0, but for the accepted specimen (Figure 8e) TRM_0 is only 6% smaller. The Zijderveld diagrams (Figure 8b and 8f) show that for a sample with larger NRM-TRM difference (i.e., dka-726) the low coercive, viscous component is much more important.

4.4. Continuous Double-Heating High-Temperature Experiments: Triaxe

[29] A total of 21 specimens with a volume of about 0.75 cm^3 have been analyzed using the continuous high-temperature magnetization measurement method, defined as the "Triaxe" technique [*Le Goff and Gallet*, 2004]. The technique involves several continuous zero field heating and cooling cycles up to a maximum temperature of 650°C with a rate of 25°C/min and one in-field cooling cycle. Magnetization was monitored through all cycles with a three-axis vibrating sample magnetometer within a Helmholtz coil system covered by a μ-metal shield. The measurement protocol is as follows: in zero field, after initial heating at T_{low}, the sample is first heated until a certain temperature T_{high}, which was in our case 300°C for most of the samples. From this curve results the NRM demagnetization, i.e., curve 1 in Figure 9b ($M_1(T)$). Then, the sample is cooled down to temperature T_{low} and heated again up to T_{high} always in zero field, which yields the temperature dependence of the residual NRM being still blocked at T_{high}, i.e., with unblocking temperatures > T_{high}; see curves 2 and 3, respectively, in Figure 9b (supplying $M_3(T)$). Subsequently, a magnetic field with known direction and intensity is applied, 40 to 50 μT along the ChRM direction in our case, and the sample is again cooled down until T_{low} which gives a TRM_{lab} acquisition, see curve 4 in Figure 9b. Next, the field is switched off and the sample is again heated until T_{high} and that is the laboratory TRM demagnetization, see curve 5 in Figure 9b (supplying $M_5(T)$). The reader is referred to *Le Goff and Gallet* [2004] and *Gallet et al.* [2006] for detailed information regarding the experimental setup and paleointensity quality assessment. It is noticed that anisotropy of TRM is automatically corrected by correcting the field orientation in order to obtain remanent magnetization in the exact NRM direction.

[30] In contrast to common Thellier experiments where the sample remanence of each temperature step is measured after cooling to room temperature, the "Triaxe" technique uses continuous remanence measurements during heating/cooling process. Con-

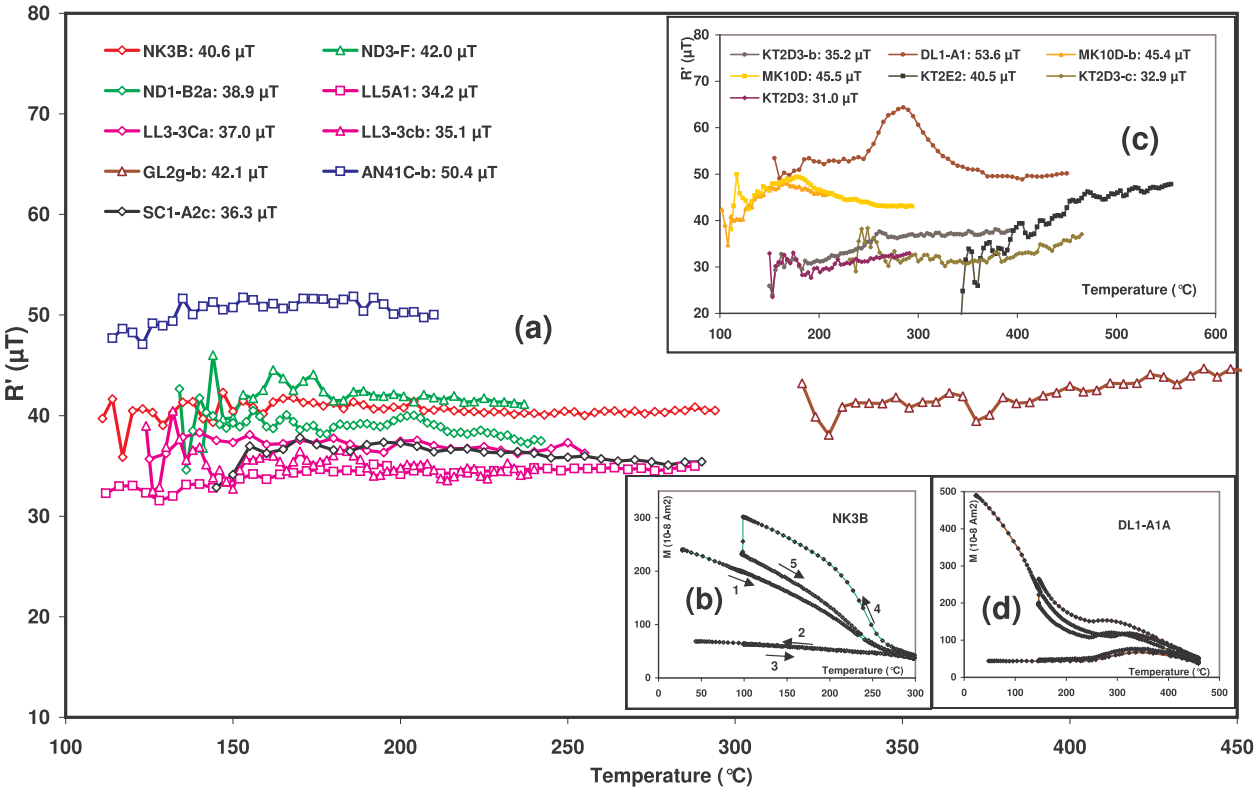

Figure 9. Summary of paleointensity determinations applying the continuous high-temperature magnetization measurement method [*Le Goff and Gallet*, 2004]. The paleointensity is defined as the mean of parameter $R'(T)$ over the used temperature range. (a) A successful experiment is indicated if $R'(T)$ remains constant over the whole range. (c) Unsuccessful specimens do show deviations. The whole set of measured magnetization curves during the experiment for (b) a successful sample and (d) a rejected sample exhibiting a self-reversal behavior. For explanation of numbered curves in Figure 9b, the reader is referred to section 4.4 or *Le Goff and Gallet* [2004, Figure 2].

sequently, both thermal demagnetization curves are $NRM(T) = M_1(T) - M_3(T)$ and $TRM_{lab}(T) = M_5(T) - M_3(T)$. The paleointensity R' in function of temperature T is proportional to the ratio between the lost parts between T_{low} *and* T, as follows

$$R'(T) = H_{lab}\frac{NRM(T_{low}) - NRM(T)}{TRM_{lab}(T_{low}) - TRM_{lab}(T)} \qquad (4)$$

We would like to draw attention on the fact that the temperature T represents discrete temperatures each 3°C or 4°C and that the $R'(T)$ should not be mistaken as the Cisowski parameter *R(H)* mentioned before in section 3.

[31] Characteristic $R'(T)$ curves are summarized in Figure 9 with two examples showing successful (Figures 9a and 9b) and unsuccessful experiments (Figure 9c). An advantage of the Triaxe technique is the possibility of detecting partial self-reversals during zero field cooling sequences (Figures 9c and 9d), induced by coexisting different mineralogical phases. This has been the case for the three specimens from flow dkl-1950 (LL3-3Ca, LL3-3cb and LL5A1). It cannot be excluded that similar mechanisms concern also other samples studied with different double-heating techniques. Since the self-reversals of the dkl-1950 samples have been observed for temperature ranges well above the segment used for paleointensity determination, they should not have affected the results. In fact, most self-reversal behavior was observed for samples that were not suitable for paleointensity determination.

[32] We used the same quality criteria as for archeological material in order to discriminate successful from unsuccessful experiments. They rely on the presence of a unidirectional NRM, a smooth shape of the $R'(T)$ curve, a slope of $R'(T)$ that is lower than 15% and that more than 50% of the NRM to be involved in the calculation of paleointensity. Nine out of the 21 measured specimens met these

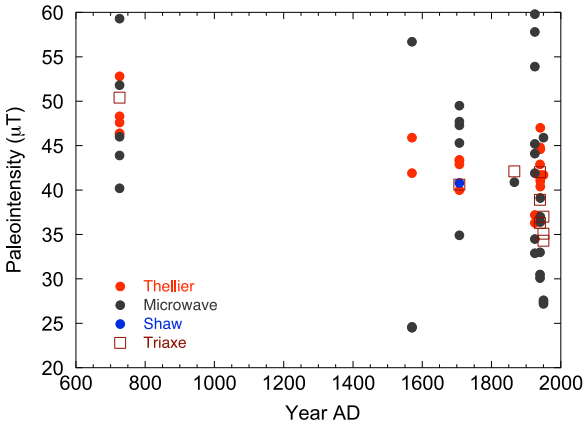

Figure 10. Paleointensity determinations obtained by each technique plotted as a function of age for the historical lava flows from Santorini.

criteria and were thus retained for calculation of absolute paleointensity.

5. Discussion

[33] All accepted individual determinations of absolute paleointensity are reported in Data Set S2 in the auxiliary material with the standard quality parameters of *Coe et al.* [1978].[1] Each individual value of absolute paleointensity has also been plotted in Figure 10 as a function of the age of the flow while the mean paleointensities derived from the different methods have been summarized in Table 3 for each lava flow. The average success rate does not strikingly vary between the different methods (Thellier: 49%, microwave: 38%, Triaxe: 42%) except for the Shaw technique (11%). The first feature emerging from Figure 10 is the large and actually similar dispersion (20–30 μT) inherent to all flows. We note that the scatter is mostly caused by the black dots which represent the microwave technique. In contrast, the results of the double heating techniques are relatively consistent for the old as well as for the young flows.

[34] The three most recent flows are young enough for testing the paleointensity estimates with respect to the field intensity provided by the geomagnetic field models [*Jackson et al.*, 2000; *Finlay*, 2008]. All field models for the period 1840–2000 are identical since they rely on the same historical measurements. The field intensity at Santorini was 42 μT in 1866, 42 μT in 1925, 43 μT in 1940, 43 μT in 1941, and 44 μT in 1950. The corresponding mean paleointensities (Figure 11) obtained from the microwave experiments (40.9 μT, 46.2 ± 8.0 μT, 31.2 ± 1.5 μT, 37.5 ± 1.4 μT and 32.1 ± 9.2 μT) are farther away from the historical field value than the other results except for the 1866 flow. The four most recent flows deviate by 10%, 27% 13% and 27% from the expected value.

[35] Compared to thermal demagnetization, most of the microwave demagnetization showed a much broader NRM unblocking range. It might be possible that the unblocking power ranges of the two magnetic phases (compare Figure 2) overlap each other, which is not ideal for paleointensity experiments. The overall intraflow dispersion inherent to the results (Figure 10) does not favor this technique, at least for these lavas.

[36] Unfortunately, we cannot provide a similar thorough test for the Shaw experiments in the absence of data for the same young flows. We note that the paleointensity obtained by this technique has been overestimated in specimens with a strong low coercive component (e.g., Figure 8b) which is not present during TRM acquisition. We infer that these changes affected the NRM/TRM ratio but were not detected by the ARM demagnetization curves, which cover a different coercivity range than those of NRM and TRM in certain specimens (e.g., Figure 8a).

[37] The paleointensity determination success rate of thermal and microwave methods is apparently not associated with mineralogical differences between the flows as evidenced from the Day diagram (Figure 3) and Table 2. However, the fact that all three Shaw experiments for flow dkm-1570 failed

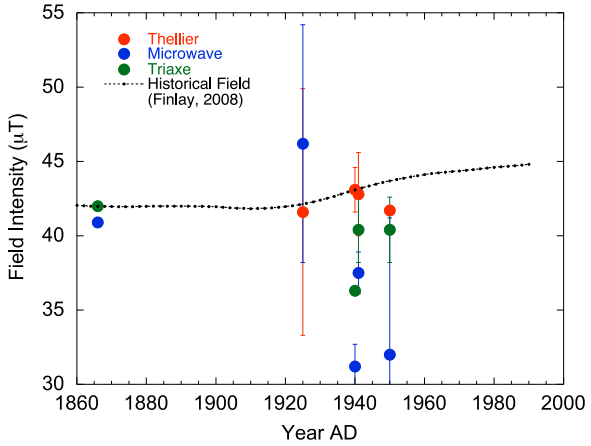

Figure 11. Mean paleointensity values obtained by the double heating (red and green dots) and the microwave techniques the historical flows erupted between 1860 and 2000 plotted along the historical field indicated by the IGRF field (10th generation) at Santorini.

[1]Auxiliary materials are available at ftp://ftp.agu.org/apend/gc/2009gc003006.

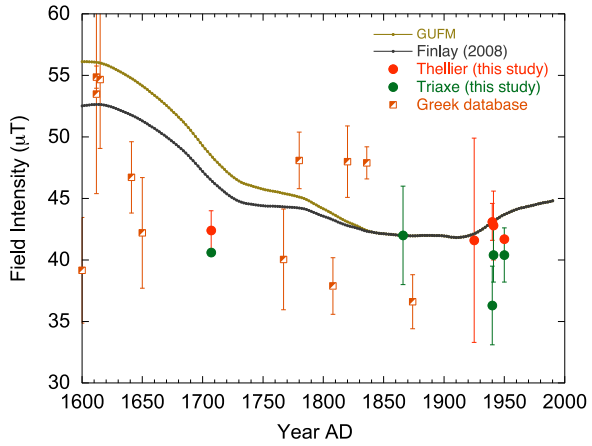

Figure 12. Paleofields derived from the Thellier and Triaxe experiments performed in this study against the Greek paleointensity database of *De Marco et al.* [2008]. All data have been reduced at the latitude of Santorini. The field intensity variations at Santorini between 1600 and 2000 A.D. predicted by the geomagnetic models of *Jackson et al.* [2000] and *Finlay* [2008] are plotted for comparison.

due to large discrepancies between NRM and TRM, is reflected in the general low H_{cr} (Table 2) for that flow.

[38] *Oishi et al.* [2005] compared the Thellier results with those from the LTD-DHT Shaw method from historical lavas from Hawaii and found that the latter yields more suitable results. The alteration experiments have shown (Figure 5) that only the 46 A.D. flow was affected by alteration. All other flows show only thermochemical alteration above 650°C, thus above the Curie temperature of the minor second magnetic mineral phase. Therefore, high-temperature oxidation was unlikely to occur during our paleointensity experiments and comparison with *Oishi et al.* [2005] is thus irrelevant.

[39] The results of the double heating experiments shown in Figures 10 and 11 appear to be more consistent within each flow. We have separated the data derived from the modified Thellier technique from those of the Triaxe measurements. The mean values obtained for each flow with a unique determination have been plotted without error bars in Figure 11. The results derived from Thellier experiments appear to be in excellent agreement with the historical field which for this period is unquestionable. We infer that the criteria used for selecting the suitable determinations are fully appropriate and yield results that lie at most 5% to 10% away from the expected field intensity.

[40] The results obtained for flows 1940 using the Triaxe are in relatively good agreement with the historical field obtained from the IGRF (10th generation). The paleofield for 1940 lies farther away but it relies on a unique determination and thus cannot be seen as a conclusive test.

[41] There appears to be a significant disagreement between the historical field of the 1950 flow and the obtained paleointensities, which is observed for all three techniques (see Figure 11). The 1950 flow, dkl-1950, has the highest H_{cr}/H_c ratio of all flows (compare Figure 3 and Table 3). This indicates that the multidomain component, i.e., the titaniferous magnetite phenocrysts and microphenocrysts < 1 mm (see section 2) with Curie temperatures > 300°C, is more pronounced than in all other flows which is confirmed by Figure 2f, where this high Curie temperature component is clearly visible in contrast to a specimen from the 1570 flow dkm-1570. Hence, we argue that the increased MD contribution in the 1950 flow causes the observed underestimation of the paleointensity. However, the specimen in Figure 2c (flow dkd-1925) shows also an enhanced high Curie temperature component, but for the 1925 flow the highest H_{cr}/H_c ratio is about 3.25 (see blue rhombi in Figure 3). Consequently, the high Curie temperature component is in this case of smaller size than for the 1950 flow.

[42] One can go further back in time and compare the obtained paleointensity results with determinations obtained in the Eastern Mediterranean area over the past 400 years after rescaling the results to the Santorini latitude. Prior to 1840, there are no historical measurements, and the models have either been calculated by using a constant decrease of the dipole at the same rate as after 1840 (GUFM model by *Jackson et al.* [2000]) or with reference to the existing archeointensity database [*Finlay*, 2008]. The most recent models [*Gubbins et al.*, 2006; *Finlay*, 2008] defend that the axial dipole term has been almost constant before 1840. A direct consequence is that the total field at Santorini is lower than in GUFM, similarly to what has recently been observed for Paris [*Genevey et al.*, 2008]. In Figure 12 we have also reported the archeointensity results obtained in the Aegean area for the past 4 centuries and recently compiled by *De Marco et al.* [2008]. Six results display lower intensities than the predictions of the models curves and 3 indicate a stronger field. The two determinations obtained in the present study for the 1707 flow are about 10% lower than the predictions. In contrast, the field estimates from *De Marco et al.* [2008] around year 1600 A.D. are consistent with those of the models. Although they

are less detailed, these features display some similarities with the picture emerging from the Paris data set [*Genevey et al.*, 2008] with lower field intensities than the predictions between 1840 A.D. and 1650 A.D. and similarly values in agreement closer to year 1600. It is obvious that additional data are necessary to further constrain the period 1590–1830 which remains documented by the ship measurements but without direct records from magnetic observatories.

6. Conclusions

[43] A detailed investigation of rock magnetic and thermochemical analysis of eight lava flows from Santorini allowed us to select a series of suitable samples for paleointensity experiments. The historical lavas contain at least two different titaniferous populations of magnetite with variable contributions to the bulk remanent magnetization. The existence of historical and recent flows was a good opportunity for comparing and testing the most widely used techniques for absolute paleointensity. Despite the fact that a different number of samples have been used for each technique we note that all success rates (except for the AF technique) are more or less equivalent. It is clear that the microwave determinations are quite scattered and not much consistent with the historical field values. Given the large number of samples measured using this technique the present test cannot be disregarded. We wonder whether this failure to reproduce the correct field value was amplified by the presence of low unblocking temperatures or whether this is the expression of a more general problem related to the correspondence between phonons and temperature. The results derived from the double heating procedures have been found in agreement with the historical field intensity provided that a sufficient number of specimens has been retained, which can be interpreted as an indication regarding the quality of the lava for these experiments. A dominant characteristic is that the natural remanent magnetization of all successful paleointensities based on double heating experiments involves samples with a single mineral (titanomagnetite in the present case) and a narrow distribution of the magnetic grain sizes consistently with experiments conducted on other historical flows from Hawaii. We infer that the existence of a sharp decrease of the NRM within a narrow range of temperatures in presence of a unique mineralogy can be considered as a promising indication for successful paleointensities in basaltic flows. Unfortunately, the results obtained between 1650 and 1900 remain too sparse to constrain the Greek archeomagnetic database during this period. We note that a similar absence of data prevailed also in the French database while this period is crucial for constraining the evolution of the dipole prior to the historical field measurements of the magnetic observatories.

Acknowledgments

[44] We wish to express our thanks to Sotiris Valkaniotis, Emanuela DeMarco, Giannis Kotiadis, and Michail Fytikas for sampling assistance and for providing field logistics and an introduction to the local geology. Ramon Egli is acknowledged for having made available his software package MAGMIX for the analysis of remanent magnetization curves. We are indebted to the staff of the Institute for Rock Magnetism, Minnesota, USA, and particularly Mike Jackson, for providing the Tiva Canyon tuff and the Wright magnetite samples for comparison. We are also grateful to John Shaw and Mimi Hill for allowing the use of the Liverpool microwave system and their succor during our microwave experiments, as well as to David Dunlop, Fabio Donadini, Catherine Kissel, John Tarduno, and an anonymous reviewer for their careful and critical reviews. D.K. acknowledges the support of the Aristotle University of Thessaloniki (Greece), which provided a 4 month grant for a research visit at the Institut de Physique du Globe de Paris (France), and S.S. acknowledges financial support of the Belgian Science Policy, project C2SPPINTENSCLIM "Bepaling van de intensiteit van het geomagnetisch veld gedurende de twee laatste millenia in België. Verband met het klimaat," as well as from project "Vallée Magnétique" supported by the Belgian Minister of Small and Medium-Sized Enterprises, Self-Employment, Agriculture and Scientific Research, S. Laruelle, and the Secretary of State for Social Affairs in Charge of Disabled People, J.-M. Delizée. This research has been enabled through the generous support of the European Commission who financed the European Research Training Network Archaeomagnetic Applications for the Rescue of Cultural Heritage (AARCH) contract HPRN-CT-2002-00219.

References

Aitken, M. J., A. L. Allsop, G. D. Bussell, and M. B. Winter (1988), Determination of the intensity of the Earth's magnetic field during archaeological times: Reliability of the Thellier technique, *Rev. Geophys.*, *26*, 3–12, doi:10.1029/RG026i001p00003.

Barton, M., and J. P. P. Huijsmans (1986), Post-caldera dacites from the Santorini volcanic complex, Aegean Sea: An example of the eruption of lavas of near constant composition over a 2200 year period, *Contrib. Mineral. Petrol.*, *94*, 472–495, doi:10.1007/BF00376340.

Böhnel, H., A. J. Biggin, D. Walton, J. Shaw, and J. A. Share (2003), Microwave palaeointensities from a recent Mexican

lava flow, baked sediments and reheated pottery, *Earth Planet. Sci. Lett.*, *6751*, 1–16.

Burov, B. V., D. K. Nourgaliev, and P. G. Jasonov (Eds.) (1986), *Palaeomagnetic Analysis* (in Russian), Kazan Univ. Press, Kazan, Russia.

Cisowski, S. (1981), Interacting vs. non-interacting single-domain behavior in natural and synthetic samples, *Phys. Earth Planet. Inter.*, *26*, 56–62, doi:10.1016/0031-9201(81)90097-2.

Coe, R. S. (1967), The determination of paleo-intensities for the Earth's magnetic field with emphasis on mechanisms which could cause non-ideal behavior in Thellier's method, *J. Geomagn. Geoelectr.*, *19*, 157–179.

Coe, R. S., S. Grommé, and E. A. Mankinen (1978), Geomagnetic paleointensities from radiocarbon-dated lava flows on Hawaii and the question of the Pacific nondipole low, *J. Geophys. Res.*, *83*, 1740–1756, doi:10.1029/JB083iB04p01740.

Cogné, J. P. (2003), PaleoMac: A Macintosh™ application for treating paleomagnetic data and making plate reconstructions, *Geochem. Geophys. Geosyst.*, *4*(1), 1007, doi:10.1029/2001GC000227.

Conticelli, S., L. Francalanci, A. P. Santo, and C. Petrone (1998), Mineral chemistry as a contribution to the understanding of the Post-Minoan magmatic system of Santorini, Greece, in *Proceedings of the Second Workshop Santorini, Greece, 2nd to 4th of May 1996*, edited by R. Casale et al., pp. 157–174, Eur. Comm., Santorini, Greece.

Cottrell, R. D., and J. A. Tarduno (2000), In search of high-fidelity geomagnetic paleointensities: A comparison of single plagioclase crystal and whole rock Thellier-Thellier analyses, *J. Geophys. Res.*, *105*, 23,579–23,594, doi:10.1029/2000JB900219.

Day, R., M. Fuller, and V. A. Schmidt (1977), Hysteresis properties of titanomagnetics: Grain-size and compositional dependence, *Phys. Earth Planet. Inter.*, *13*, 260–267, doi:10.1016/0031-9201(77)90108-X.

Dekkers, M. J., and H. Böhnel (2006), Reliable absolute palaeointensities independent of magnetic domain state, *Earth Planet. Sci. Lett.*, *248*, 507–516, doi:10.1016/j.epsl.2006.05.040.

De Marco, E. (2007), Integrated magnetic and archeomagnetic measurements in archeological sites: Contribution to secular variation curves for Greece, Ph.D. thesis, Aristotle Univ. of Thessaloniki, Thessaloniki, Greece.

De Marco, E., V. Spatharas, M. Gómez-Paccard, A. Chauvin, and D. Kondopoulou (2008), New archaeointensity results from archaeological sites and variation of the geomagnetic field intensity for the last 7 millennia in Greece, *Phys. Chem. Earth*, *33*, 578–595.

Donadini, F., M. Kovacheva, M. Kostadinova, L. Casas, and L. J. Pesonen (2007), New archaeointensity results from Scandinavia and Bulgaria: Rock-magnetic studies inference and geophysical application, *Phys. Earth Planet. Inter.*, *165*, 229–247, doi:10.1016/j.pepi.2007.10.002.

Downey, W. S., and D. H. Tarling (1984), Archaeomagnetic dating of Santorini volcanic eruptions and fired destruction levels of the Late Minoan civilization, *Nature*, *209*, 509–523.

Druitt, T. H., L. Edwards, R. M. Mellors, D. M. Pyle, R. S. J. Sparks, M. Lanphere, M. Davies, and B. Barreirio (Eds.) (1999), *Santorini Volcano*, *Geol. Soc. Mem.*, vol. 19, 176 pp., Geol. Soc., London.

Dunlop, J. D. (2002), Theory and application of the Day plot (M_{rs}/M_s versus H_{cr}/H_c): 1. Theoretical curves and tests using titanomagnetite data, *J. Geophys. Res.*, *107*(B3), 2056, doi:10.1029/2001JB000486.

Dunlop, J. D., and Ö. Özdemir (1997), *Rock Magnetism, Fundamentals and Frontiers*, 573 pp., Cambridge Univ. Press, Cambridge, U. K.

Egli, R. (2003a), Analysis of the field dependence of remanent magnetization curves, *J. Geophys. Res.*, *108*(B2), 2081, doi:10.1029/2002JB002023.

Egli, R. (2003b), Environmental influences on the magnetic properties of lake sediments, Ph.D. thesis, 253 pp., ETH Zurich, Zurich, Switzerland.

Fabian, K., and T. von Dobeneck (1997), Isothermal magnetization of samples with stable Preisach function: A survey of hysteresis, remanence and rock magnetic parameters, *J. Geophys. Res.*, *102*, 17,659–17,677, doi:10.1029/97JB01051.

Finlay, C. C. (2008), Historical variation of the geomagnetic axial dipole, *Phys. Earth Planet. Inter.*, *170*, 1–14, doi:10.1016/j.pepi.2008.06.029.

Francalanci, L., G. Vougioukalakis, G. Elefteriades, L. Pinarelli, C. Petrone, P. Mantetti, and G. Christofides (1998), Petrographic, chemical and isotopic variations in the intra-caldera post-Minoan rocks of the Santorini volcanic field, in *Proceedings of the second workshop Santorini, Greece, 2nd to 4th of May 1996*, edited by R. Casale et al., pp. 175–186, Eur. Comm., Santorini, Greece.

Friedrich, W. L., B. Kromer, M. Friedrich, J. Heinemeier, T. Peiffer, and S. Talamo (2006), Santorini eruption radiocarbon dated to 1627–1600 B.C., *Science*, *312*, 548, doi:10.1126/science.1125087.

Fytikas, M., N. Kolios, and G. Vougioukalakis (1990), Post-Minoan volcanic activity of the Santorini volcano. Volcanic hazard and risk, forecasting possibilities, in *Thera and the Aegean World III*, *Earth Sciences*, vol. 2, edited by D. A. Hardy et al., pp. 183–198, Thera Found., London.

Gallet, Y., A. Genevey, M. Le Goff, F. Fluteau, and S. A. Eshraghi (2006), Possible impact of the Earth's magnetic field on the history of ancient civilizations, *Earth Planet. Sci. Lett.*, *246*, 17–26, doi:10.1016/j.epsl.2006.04.001.

Genevey, A., Y. Gallet, C. G. Constable, M. Korte, and G. Hulot (2008), ArcheoInt: An upgraded compilation of geomagnetic field intensity data for the past ten millennia and its application to the recovery of the past dipole moment, *Geochem. Geophys. Geosyst.*, *9*, Q04038, doi:10.1029/2007GC001881.

Gubbins, D., A. L. Jones, and C. C. Finlay (2006), Fall in Earth's magnetic field is erratic, *Science*, *312*, 900–902, doi:10.1126/science.1124855.

Hartstra, R. L. (1982), Grain-size dependence of initial susceptibility and saturation magnetization-related parameters of four natural magnetites in the PSD-MD range, *Geophys. J. R. Astron. Soc.*, *71*, 477–495.

Herrero-Bervera, E., and J.-P. Valet (2005), Absolute paleointensity and reversal records from the Waianae sequence (Oahu, Hawaii, USA), *Earth Planet. Sci. Lett.*, *234*, 279–296, doi:10.1016/j.epsl.2005.02.032.

Herrero-Bervera, E., and J.-P. Valet (2009), Testing determinations of absolute paleointensity from the 1955 and 1960 Hawaiian flows, *Earth Planet. Sci. Lett.*, *287*, 420–433, doi:10.1016/j.epsl.2009.08.035.

Hill, M. J., and J. Shaw (1999), Paleointensity results for historic lavas from Mt. Etna using microwave demagnetization/remagnetization in a modified Thellier type experiment, *Geophys. J. Int.*, *139*, 583–590, doi:10.1046/j.1365-246x.1999.00980.x.

Hill, M. J., and J. Shaw (2000), Magnetic field intensity study of the 1960 Kilauea lava flow, Hawaii, using the microwave paleointensity technique, *Geophys. J. Int.*, *142*, 487–504, doi:10.1046/j.1365-246x.2000.00164.x.

Jackson, A., A. R. T. Jonkers, and M. Walker (2000), Four centuries of geomagnetic secular variation from historical records, *Philos. Trans. R. Soc. London, Ser. A*, *358*, 957–990, doi:10.1098/rsta.2000.0569.

Jackson, M., P. Sølheid, B. Carter-Stiglitz, J. Rosenbaum, and J. Till (2004), Tiva Canyon Tuff (I), *IRM Q.*, *14*(3), 9–11.

Jasonov, P. G., D. K. Nourgaliev, B. V. Burov, and F. Heller (1998), A modernized coercivity spectrometer, *Geol. Carpathica*, *49*, 224–225.

Jonkers, A. R. T., A. Jackson, and A. Murray (2003), Four centuries of geomagnetic data from historical records, *Rev. Geophys.*, *41*(2), 1006, doi:10.1029/2002RG000115.

Kissel, C., and C. Laj (2004), Improvements in procedure and paleointensity selection criteria (PICRIT- 03) for Thellier and Thellier determinations: Applications to Hawaiian basaltic long cores, *Phys. Earth Planet. Inter.*, *147*, 155–169, doi:10.1016/j.pepi.2004.06.010.

Kono, M., and N. Ueno (1977), Paleointensity determination by a modified Thellier method, *Phys. Earth Planet. Inter.*, *13*, 305–314, doi:10.1016/0031-9201(77)90114-5.

Le Goff, M., and Y. Gallet (2004), A new three-axis vibrating sample magnetometer for continuous high-temperature magnetization measurements: Applications to paleo- and archeointensity determinations, *Earth Planet. Sci. Lett.*, *229*, 31–43, doi:10.1016/j.epsl.2004.10.025.

Leonhardt, R., and H. C. Soffel (2002), A reversal of the Earth's magnetic field recorded in mid-Miocene lava flows of Gran Canaria: Paleointensities, *J. Geophys. Res.*, *107*(B11), 2299, doi:10.1029/2001JB000949.

McClelland, E., and T. H. Druitt (1989), Palaeomagnetic estimation of emplacement temperatures of pyroclastic deposits on Santorini, Greece, *Bull. Volcanol.*, *51*, 16–27, doi:10.1007/BF01086758.

Oishi, Y., H. Tsunakawa, N. Mochizuki, Y. Yamamoto, K. Wakabayashi, and H. Shibuya (2005), Validity of the LTD-DHT Shaw and Thellier paleointensity methods: A case study of the Kilauea 1970 lava, *Phys. Earth Planet. Inter.*, *149*, 243–257, doi:10.1016/j.pepi.2004.10.009.

Papazachos, B. C., and D. G. Panagiotopoulos (1993), Normal faults associated with volcanic activity and deep rupture zones in the southern Aegean volcanic arc, *Tectonophysics*, *220*, 301–308, doi:10.1016/0040-1951(93)90237-E.

Petrova, G. N., and O. L. Bagina (1976), A non-thermal method of determining the intensity of the ancient geomagnetic field, *Izv. Earth Phys.*, *4*, 54–62.

Rolph, T. C., and J. Shaw (1985), A new method of palaeofield magnitude correction and its application to Lower Carboniferous lavas, *Geophys. J. R. Astron. Soc.*, *80*, 773–781.

Selkin, P., and L. Tauxe (2000), Long-term variations in paleointensity, *Philos. Trans. R. Soc. London, Ser. A*, *358*, 1065–1088, doi:10.1098/rsta.2000.0574.

Shaw, J. (1974), A new method of determining the magnitude of the palaeomagnetic field: Application to five historic lavas and five archaeological samples, *Geophys. J. R. Astron. Soc.*, *39*, 133–141.

Spassov, S., and J. Hus (2006), Estimating baking temperatures in a Roman pottery kiln by rock magnetic properties: Implications of thermochemical alteration on archaeointensity determinations, *Geophys. J. Int.*, *167*, 592–604, doi:10.1111/j.1365-246X.2006.03114.x.

Tanaka, H., and M. Kono (1984), Analysis of the Thellier-method of paleointensity determination. 2. Applicability to high and low magnetic fields, *J. Geomagn. Geoelectr.*, *36*, 285–297.

Tarduno, J. A., D. R. Cottrell, and A. V. Smirnov (2006), The paleomagnetism of single silicate crystals: Recording geomagnetic field strength during mixed polarity intervals, superchrons, and inner core growth, *Rev. Geophys.*, *44*, RG1002, doi:10.1029/2005RG000189.

Tarling, D. H., and W. S. Downey (1989), Archaeomagnetic results from late Minoan destruction levels on Crete and the Minoan tephra on Santorini, in *Thera and the Aegean World III*, *Earth Sciences*, vol. 2, edited by D. A. Hardy et al., pp. 149–159, Thera Found., London.

Thellier, E., and O. Thellier (1959), Sur l'intensité du champ magnétique terrestre dans le passé historique et géologique, *Ann. Geophys.*, *15*, 285–376.

Tsunakawa, H., and Y. Yamamoto (1999), Paleointensity measurement of the Hawaiian 1960 lava and its implications for the reliability of paleointensity determinations, *Eos Trans. AGU*, *80*(46), Fall Meet. Suppl., Abstract F300-301.

Tsunakawa, H., K. Shimura, and Y. Yamamoto (1997), Application of double heating technique of the Shaw method to the Brunhes epoch volcanic rocks, paper presented at 8th Scientific Assembly, Int. Assoc. of Geomagn. and Aeron., Uppsala, Sweden.

Valet, J.-P. (2003), Time variations in geomagnetic intensity, *Rev. Geophys.*, *41*(1), 1004, doi:10.1029/2001RG000104.

Valet, J.-P., E. Tric, E. Herrero-Bervera, L. Meynadier, and J. P. Lockwood (1998), Absolute paleointensity from Hawaiian lavas younger than 35 ka, *Earth Planet. Sci. Lett.*, *161*, 19–32, doi:10.1016/S0012-821X(98)00133-2.

Walton, D., J. Shaw, J. A. Share, and J. Hakes (1992), Microwave demagnetization, *J. Appl. Phys.*, *71*, 1549–1551, doi:10.1063/1.351230.

Walton, D., J. A. Share, T. C. Rolph, and J. Shaw (1993), Microwave magnetization, *Geophys. Res. Lett.*, *20*, 109–111, doi:10.1029/92GL02782.

Wright, J. V. (1978), Remanent magnetism of poorly sorted rock deposits from the Minoan eruption of Santorini, *Bull. Volcanol.*, *41*, 131–135, doi:10.1007/BF02597026.

Yamamoto, Y., H. Tsunakawa, and H. Shibuya (2003), Paleointensity study of the Hawaiian 1960 lava: Implications for possible causes of erroneously high intensities, *Geophys. J. Int.*, *153*, 263–276, doi:10.1046/j.1365-246X.2003.01909.x.

Yu, Y., L. Tauxe, and A. Genevey (2004), Toward an optimal geomagnetic field intensity determination technique, *Geochem. Geophys. Geosyst.*, *5*, Q02H07, doi:10.1029/2003GC000630.

Zellmer, G. F. (1998), Petrogenetic processes and their timescales beneath Santorini, Aegean volcanic arc, Greece, Ph.D. thesis, Open Univ., Milton Keynes, U. K.